ME 4041 Computer Graphics and Computer-Aided Design

Project Final Report

Remote All Terrain Fire Fighter

Yash Agarwal

Nalin Verma

Shaurya Singh

Table of Contents

INTRODUCTION

The product that is designed is a portable, all-terrain, remote-controlled robot, which is a fire analysis and retardant system. It will help firefighters by going inside a building that is structurally un-stable, may have harmful chemicals or might be thermally unsafe for firefighters to enter, by returning air samples and analyzing temperature distribution. The robot has tracks with each hub having individual suspensions, and the tracks on either side having their own individual motors. The strength is provided by a metal cage, which is covered by heat insulating material in order to protect the electronics inside. An infrared camera for high risk element detection is also incorporated. A water pipe connected to the fire hydrant is carried by the robot. This water, apart from extinguishing the fire, is also used to cool the heat sinks of the electronics.

There are several reasons to consider the application of such a product. One of the major reasons would be the danger associated with the job of a fireman. In a situation of uncontrolled fire, a scenario can change drastically often resulting from elements that were not perceived from the outside. In the case of a chemical fire, there are inflammable chemical silos which spontaneously catch fire and explode. This particular occurrence can not only kill a fireman due to expanding gases but also from structural collapse. The successful implementation of this product in the routines of combatting a fire-hazard situation would enhance the workmanship of firemen, thereby, helping save numerous lives. Currently, no production or concept robots provide feedback of the environment to the firemen. In addition, autonomous robots add an unnecessary degree of complexity to the design of robot firefighters. A human firefighter will be better trained and can take intelligent decisions.

The Remote All-Terrain Fire Fighter would be used to scientifically aid the job of a fireman by providing critical fire-situation analysis. Hence, the target market would consist of

the Fire Departments across the globe. Moreover, miniature versions of our product could be used in fire-hazard situations on aircraft carriers and other such areas, where human intervention is very difficult.

OBJECTIVES

One of the main design objectives was to have the dimensions of the structure as 4ft X 3ft X 4ft, considering that an average door is 4ft wide. The ideal weight for this machine is 120 kg so that the robot does not collapse under its own weight. Other design objectives were that the robot should have the ability to navigate through rough terrain, should be able to sustain high temperatures, and be rigid enough to sustain damage occurring from explosions and collapsing structures. Moreover, a preliminary analysis was done to get certain design parameters. The torque required for the motor was calculated to be 120 Nm. The calculated required gear ratio to achieve the desired torque was 10:1. With a maximum allowable ground pressure of 15 psi, the minimum area of contact for the robot was determined as 0.1 m^2.

MODELING

Camera Assembly

The camera assembly consists of the lens and the lens housing, the rotation housing, gears and driving motors comprising the rotation mechanism, and a mounting part. All parts were assembled using various assembly constraints such as touch align, parallel, concentric, perpendicular, etc. The camera is intended to perform high-risk element detection, and collect data regarding temperature distribution to aid firefighters in a fire-hazard situation. Figure MA1 depicts the camera assembly.

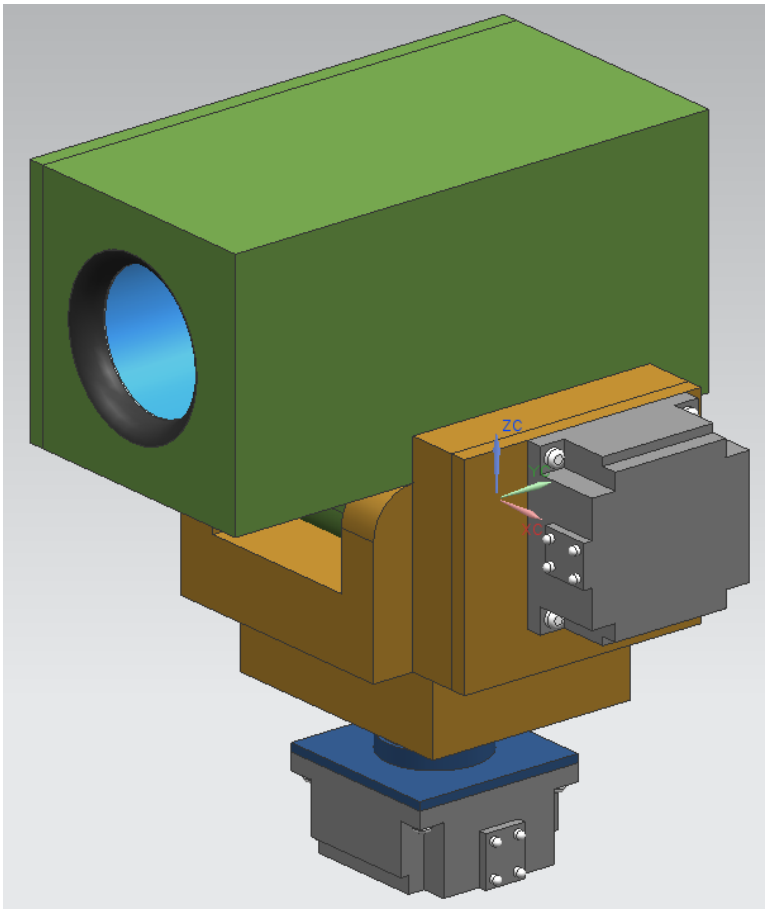

Figure MA1. Camera Assembly

Lens and Lens Housing

The lens was created using a cylindrical extrusion as shown in Figure MA2.

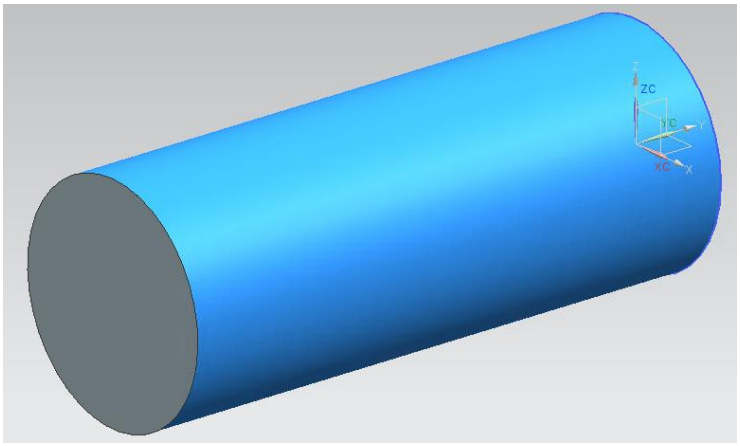

Figure MA2. Cylindrical Extrusion for the lens

A subtract extrusion was done on the front face of the lens to create the lens holder. An edge blend was also used to curve the edge of the lens holder and mimic actual lenses. These features are displayed in Figure MA3 below.

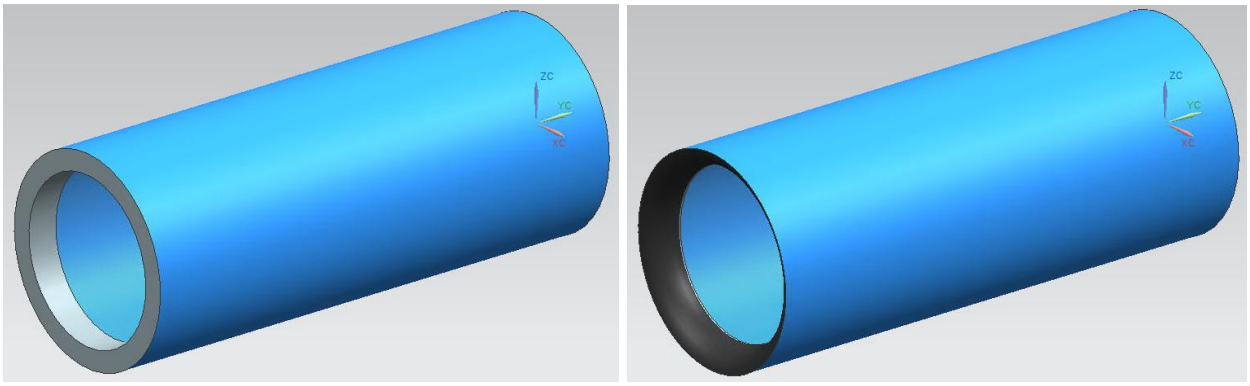

Figure MA3. Lens

The lens housing consists of a box type structure to hold the lens in place. It was created using the extrude command, and then using the shell command to create a wall thickness for the box. The pattern feature command was used to create holes on the wall for screws. A hole was also extruded with the same circular dimension as that of the lens to fit the lens in place. Lastly, a feature at the bottom was extruded to mount the lens housing on the rotation housing. The edge blend command was also used to give a radial clearance to the bottom feature for maximum rotation of the lens housing in the vertical direction. Figure MA4 depicts the modeling of the lens housing.

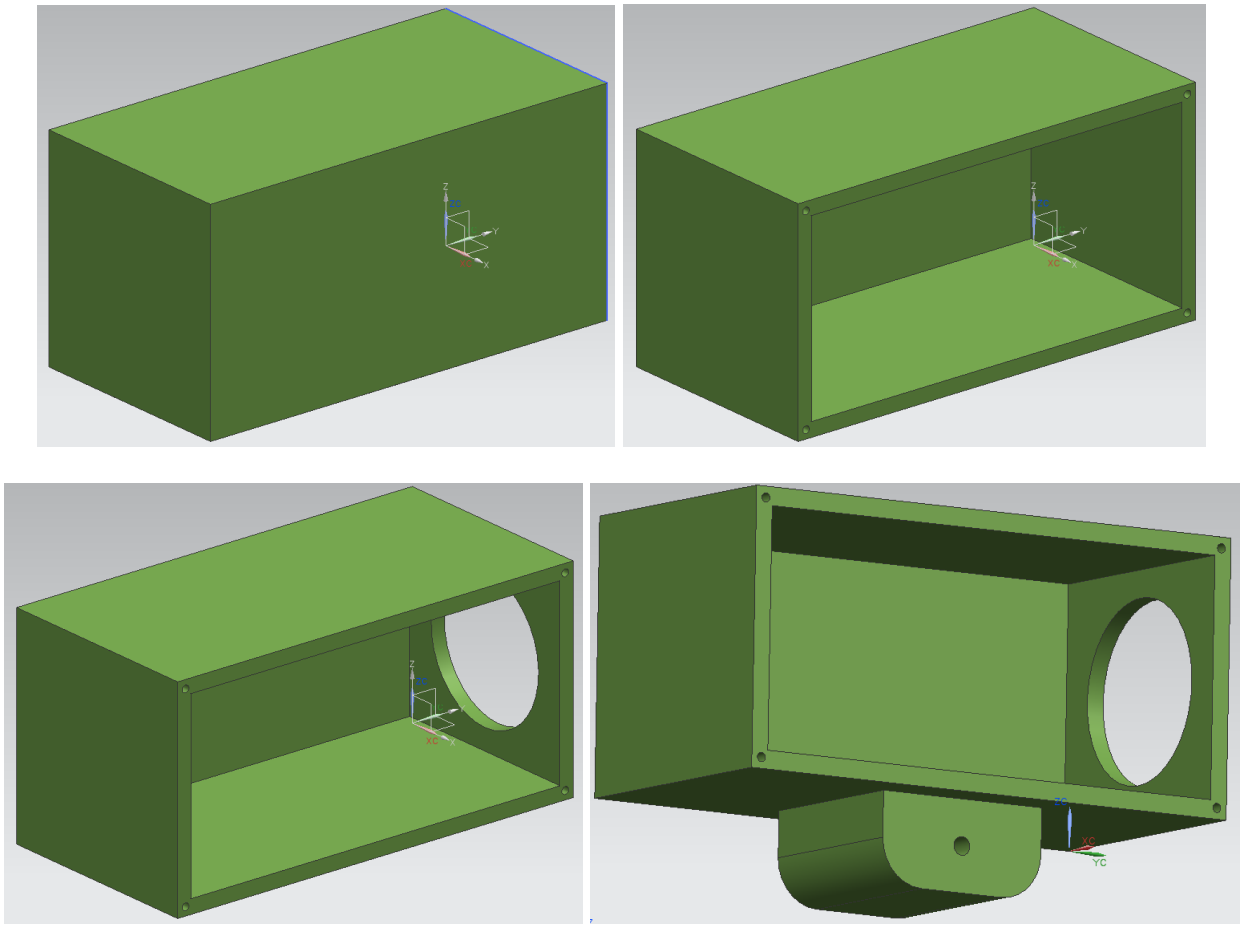

Figure MA4. Lens Housing

Figure MA5 displays the assembled lens and lens housing. A lens housing cover is also depicted in the figure.

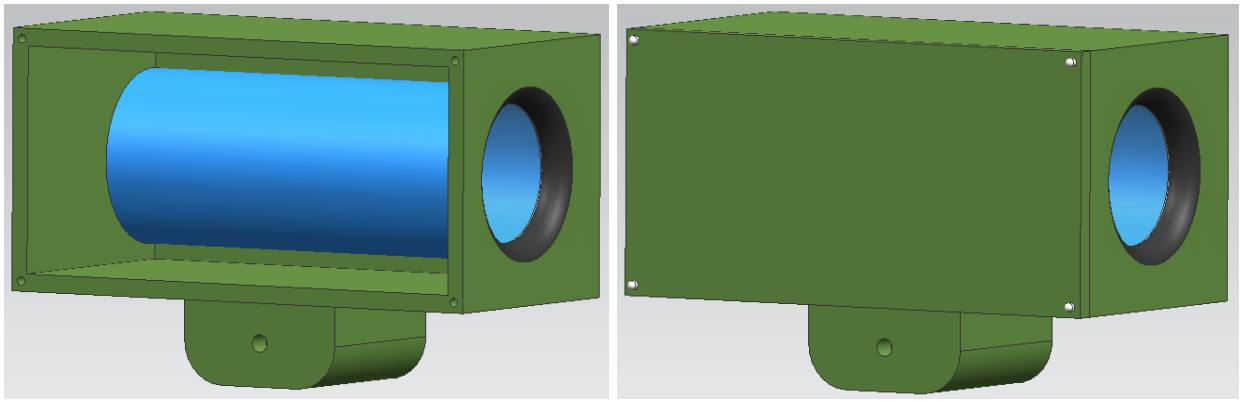

Figure MA5. Assembled Lens and Lens Housing

Rotation Housing

The rotation housing is the part to which the lens housing is mounted. It consists of one gear box on the side and one at the bottom for vertical and horizontal rotation of the camera. The extrude command was used in two ways, addition and subtraction, to get the desired shape. The edge blend command was also used to avoid sharp edges on it. Moreover, the shell command was used to provide a wall thickness on the gear box. Figure MA6 depicts the modeling of the rotation housing.

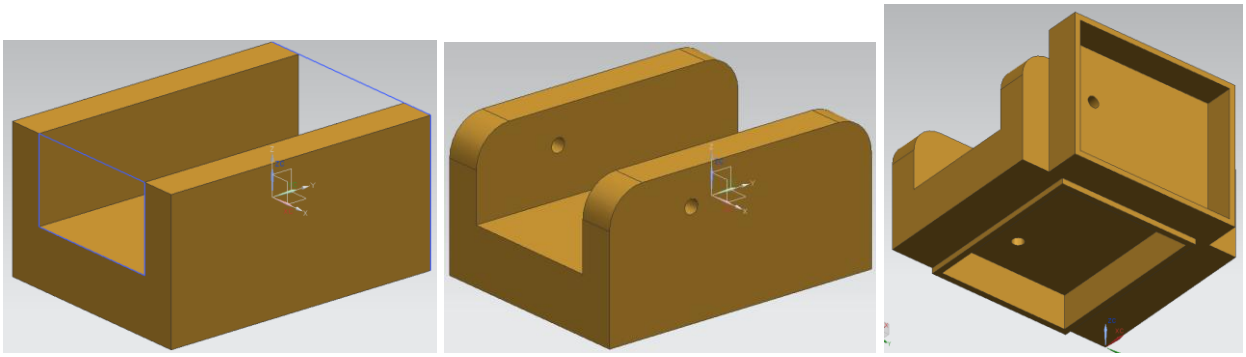

Figure MA6. Rotation Housing

Gears and Driving Motor

The gears are used for vertical and horizontal rotation of the camera assembly. The gears are housed in the gearbox, and connected with shafts to two driving motors. The gear was modeled using the extrude command and pattern feature command for the teeth. The shaft was extruded using the extrude command. The driving motor was modeled using a standard sketch used for extrusion, after which subtract extrusions were made on the corners to accommodate for screws. Figures MA7 and MA8 depict the modeling process for the gear and the driving motor, respectively.

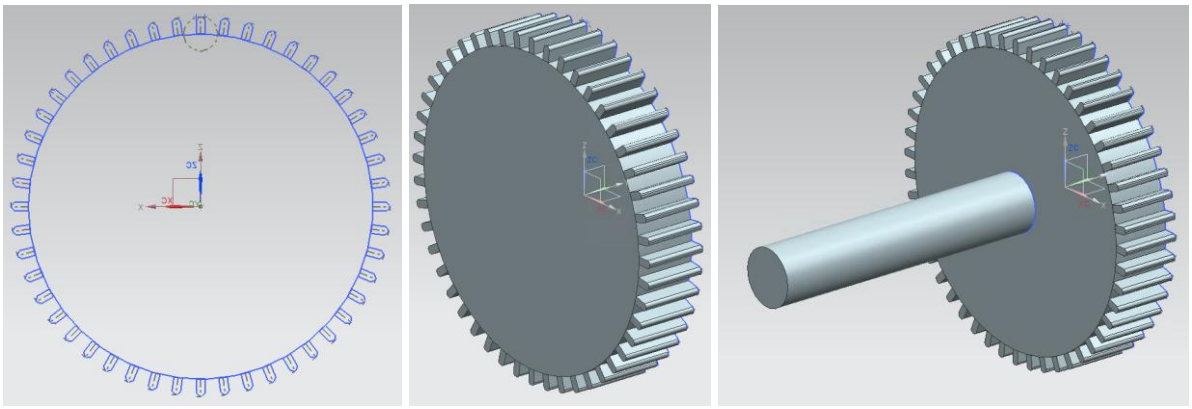

Figure MA7. Gear

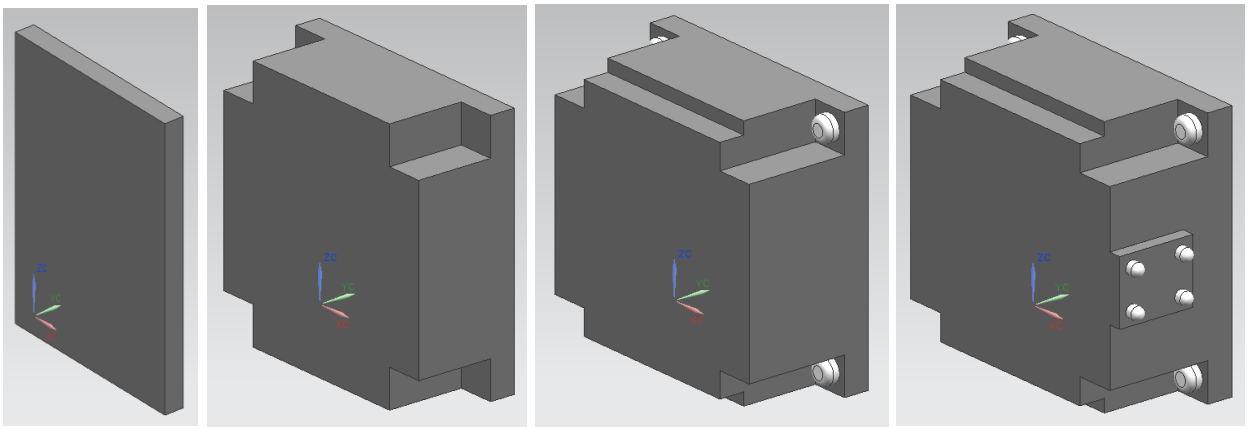

Figure MA8. Driving Motor

The gear and the driving motor assembly on the rotation housing is shown below.

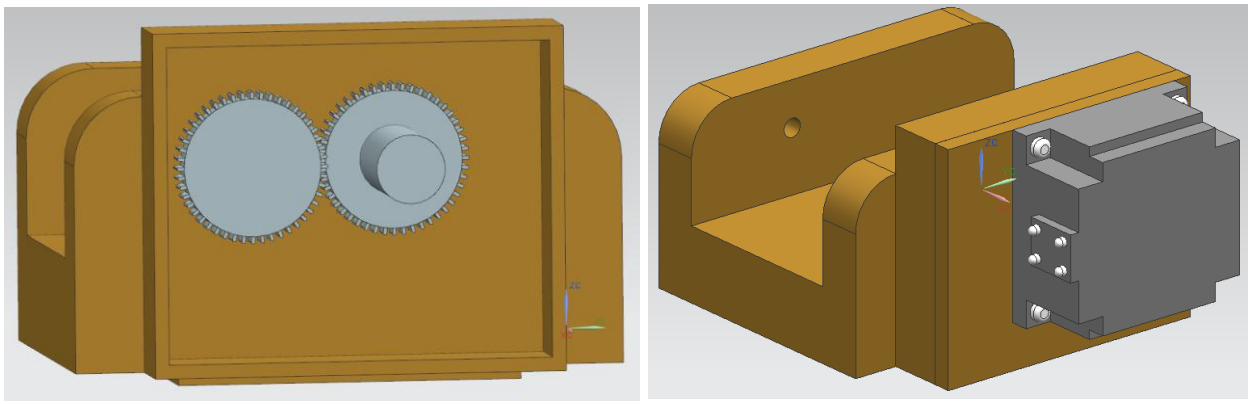

Figure MA9. Gears and Motor on Rotation Housing

Mounting Part

The mounting part is connected at the bottom. This part is used to mount the camera assembly to the robot. Figure MA10 shows the mounting part. Also, a circular indentation in the middle of the mounting part was created, so as to provide for controlled rotation in the horizontal direction, while being stationary with respect to the robot.

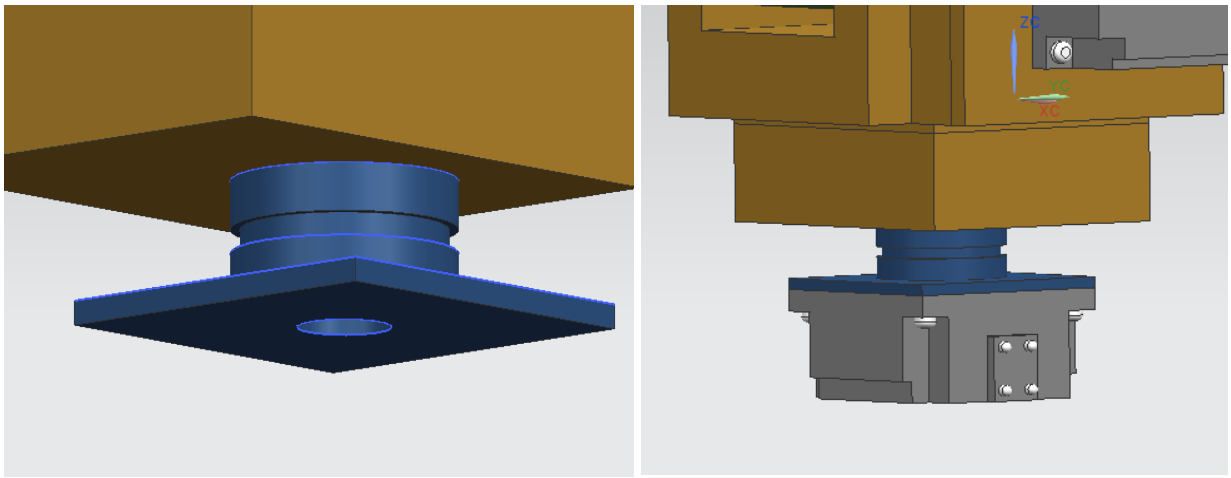

Figure MA10. Mounting Part

Electronics Cooling Assembly

The electronics cooling assembly consists of the water hose, heat sink and electronics. All parts were assembled using various assembly constraints such as touch align, parallel, concentric, perpendicular, etc. The electronics in the robot are cooled using fins. The heat generated from the electronics is conducted to the fins, which loses the heat to water flowing over them through convection. A steady state is obtained over time, which keeps the temperature of the electronics at a constant 40℃. Figure MB1 below depicts this assembly.

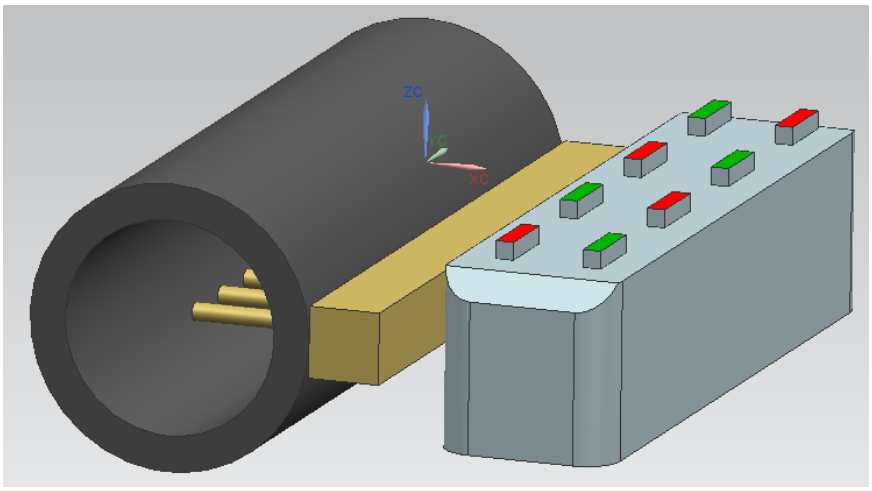

Figure MB1. Electronics Cooling Assembly

Water Hose

A water hose connected to the fire hydrant is carried by the robot. This water, apart from extinguishing the fire, is also used to cool the heat sinks of the electronics. Apart from the extrude and shell commands used as in earlier parts discussed, a new modeling technique was used for the water hose. The holes on the side of the hose used for the heat sink, were modeled by offsetting a datum plan to the side of the hose, since a sketch cannot be directly made on the circular surface of a cylinder. Figure MB2 depicts the modeling process of the hose.

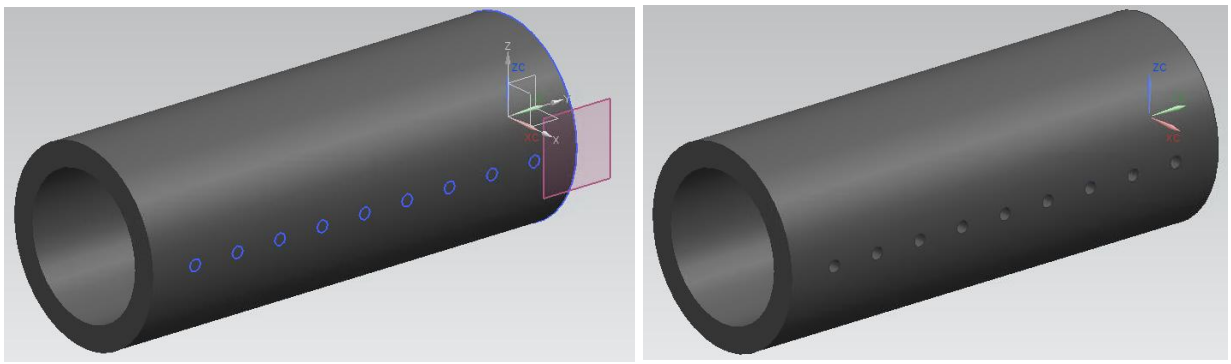

Figure MB2. Water Hose

Heat Sink

The heat sink was designed to concentrically fit inside the water hose. The pattern curve command was used while making the sketch for the part, after which it was extruded. Figure MB3 shows the modeling process for the heat sink.

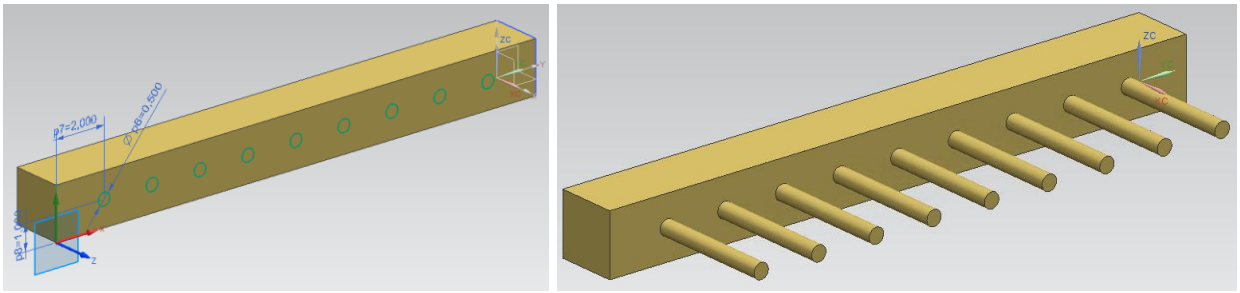

Figure MB3. Heat Sink

Electronics

The electronics in this project were not modeled in an aesthetic manner. More emphasis was given to the mechanical criteria, and hence, the electronics were modeled as a structure having rectangular extrusions. The red and green extrusions are considered to be the different kinds of electronics, depicted by Figure MB4.

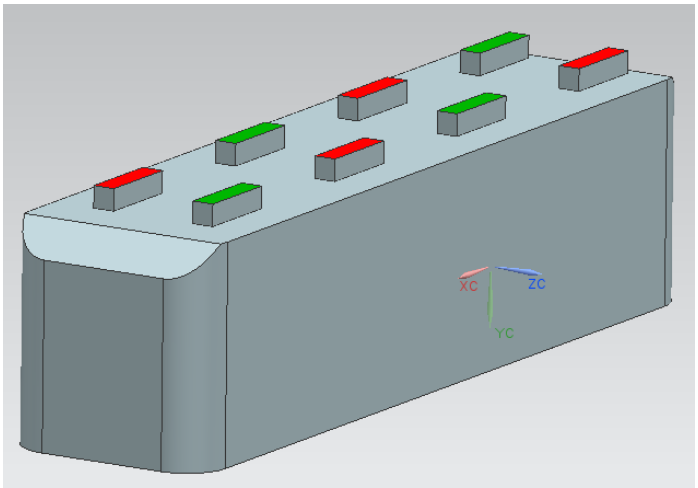

Figure MB4. Electronics

Drive System Assembly

The drive system assembly consists of motor, gear box, and tracks, as illustrated in Figure MC0.

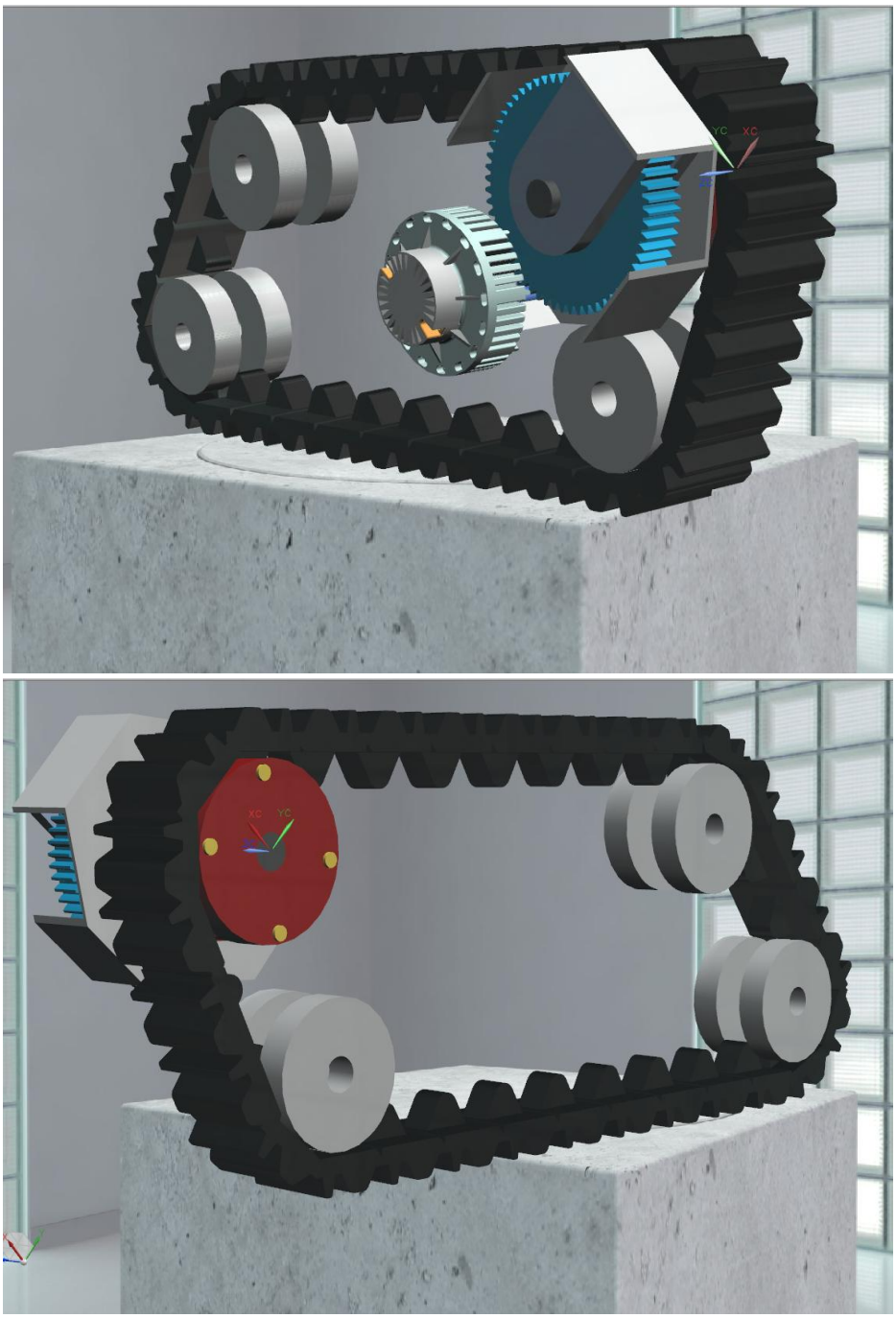

Figure MC0. Drive System Assembly

Gear box modeling

After the analysis for the gearbox was completed, the gear ratio to be modeled was found to be 10:1. This is in order to increase the torque from the motor from 20.5 Nm to 205 Nm. As the robot will not be required to different torques and maximum speeds, the simplified gear system will be implemented. This gear system will only utilize two gears with teeth ratio 10:1. The modeling of the gears required additional challenge as there are a lot of variables like diametral pitch, number of teeth, face width and pressure angle. The most commonly used gears were looked up and found that spur gear will be sufficient in this application as the helical gears provided unnecessary complexity. The pressure angle was selected to be 20 degrees and face width to be 5 in. The diametral pitch was set at 5 and this was kept constant between all gears as it is necessary for smooth operation. After setting the number of teeth to 100, the gear was modeled by calculating the pitch diameter, base diameter and addendum. The calculated pitch came about to be 12 in. The base diameter was calculated to be 11.3 in. The large drive shaft diameter (large gear) was chosen to be 2 in. and small drive shaft diameter (small gear) was chosen to be 1 in. Figures MC1-MC3 illustrate the modeling process:

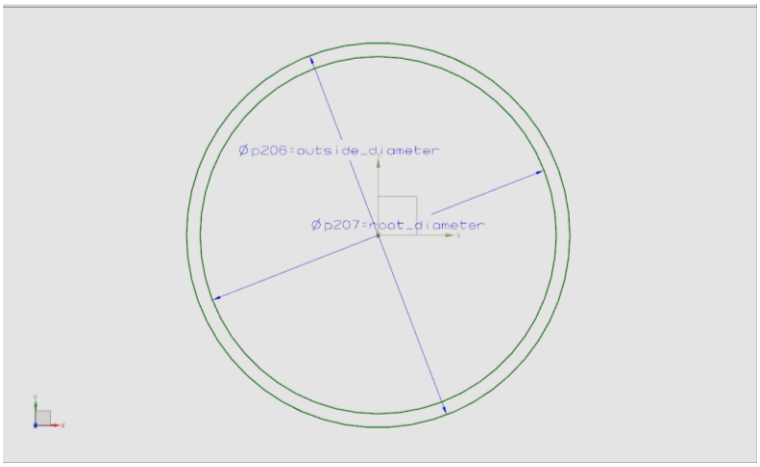

MC1. The gear geometry

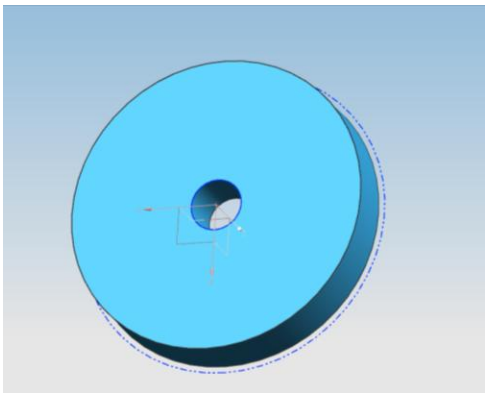

MC2. Extruded gear geometry with pitch diameter displayed

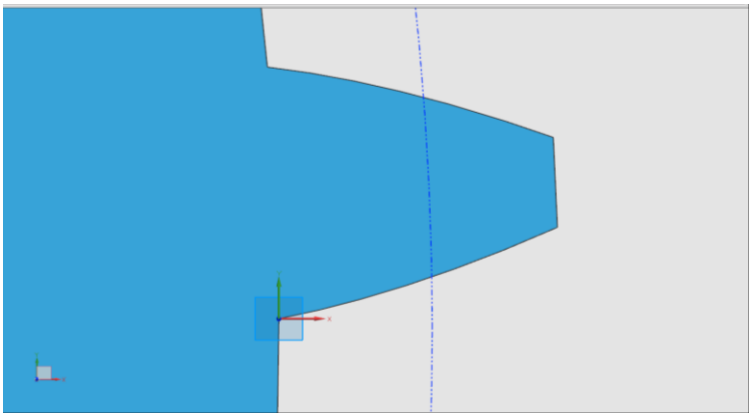

MC3. Extruded gear element from the calculated dimensions

Next, the gear element was patterned using Count and Span feature. The span was 360 degrees and count was 100. The final component is shown in Figure MC4.

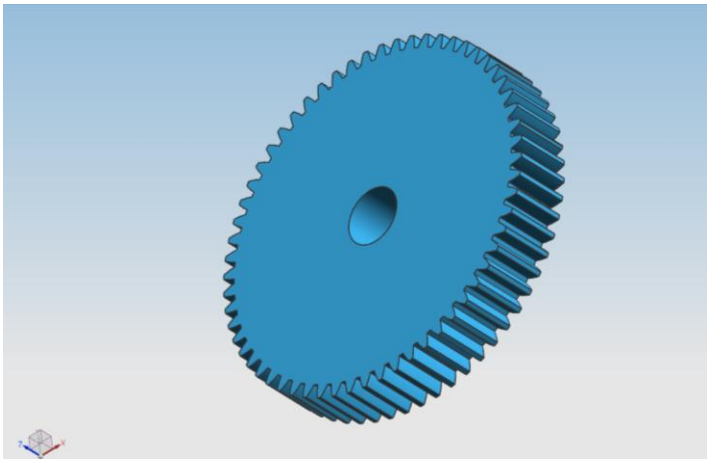

MC4. Final larger gear

Next, the smaller gear was designed using the same calculated dimensions but with 10 teeth. Illustrations are shown in Figures MC5-MC6:

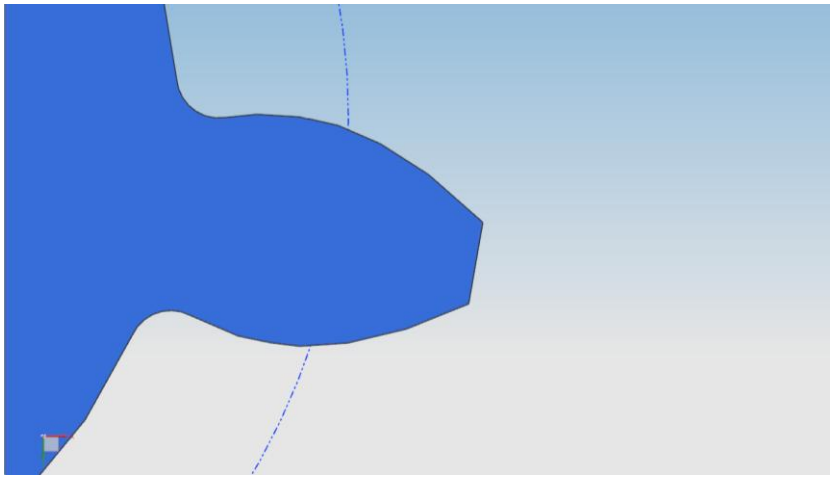

MC5. Smaller gear profile with additional Edge Blends

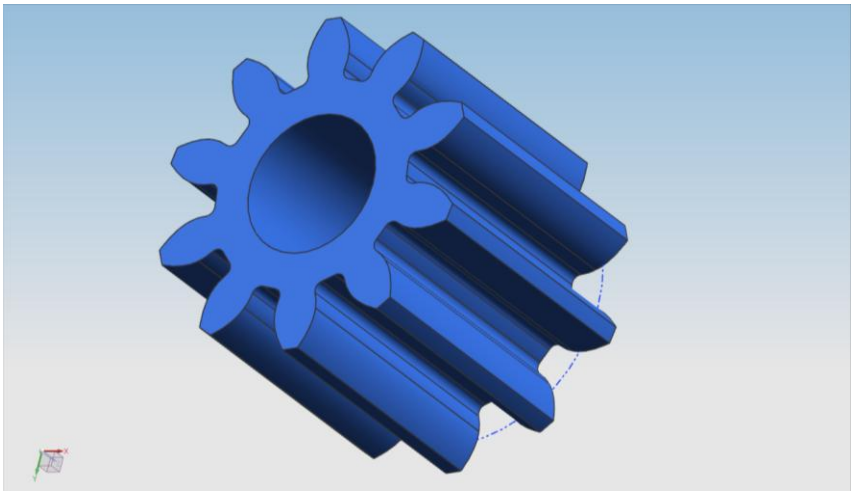

MC6. Patterned gear profiles

Next, the mounts for the gears in the gearbox were modeled. The total length of the gearbox was calculated based on the assembly of the two gears. The length was found to be 14 in. but an additional 1 in clearance was provided at either end, making it to 16 in. The width was chosen to be 14 in. as the diameter of the larger gear and the clearance was added. The thickness

was chosen to be 6 in. using the same criterion. The shelling, however, decreased 0.5 in. of clearance; this was deemed acceptable. The modeling process is shown in Figures MC7-MC11:

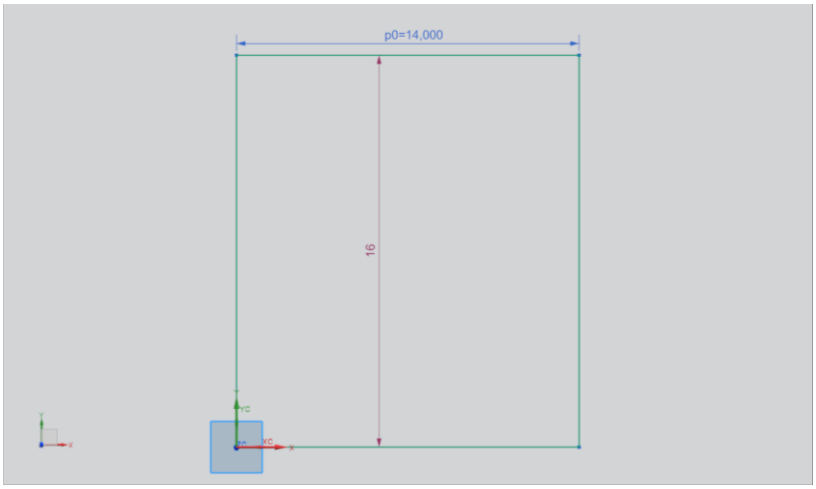

MC7. Sketch for gearbox

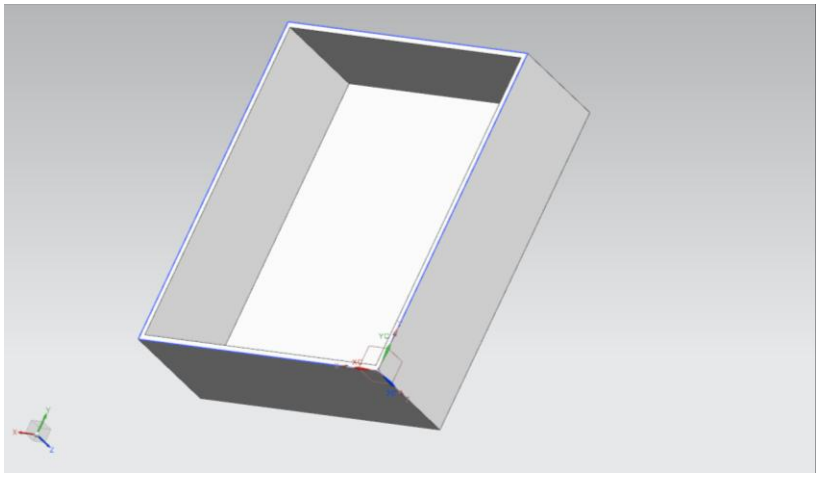

MC8. Extruded and shelled gearbox

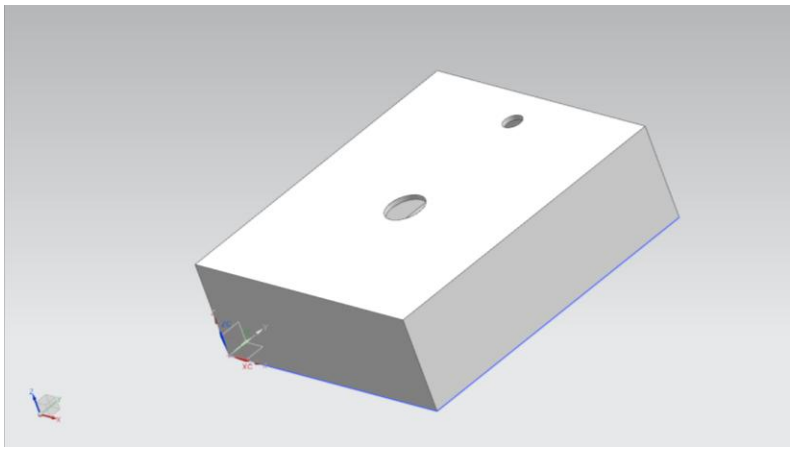

MC9. Hole feature was used to bore holes for drive shafts

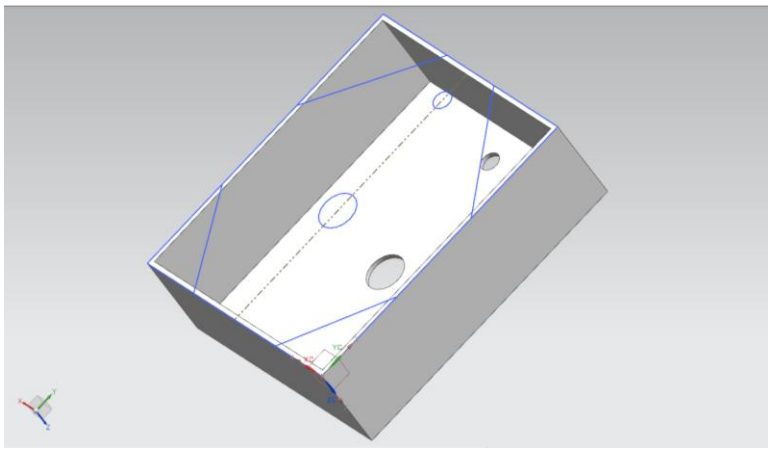

MC10. The excess corners were trimmed off using Extrude subtraction

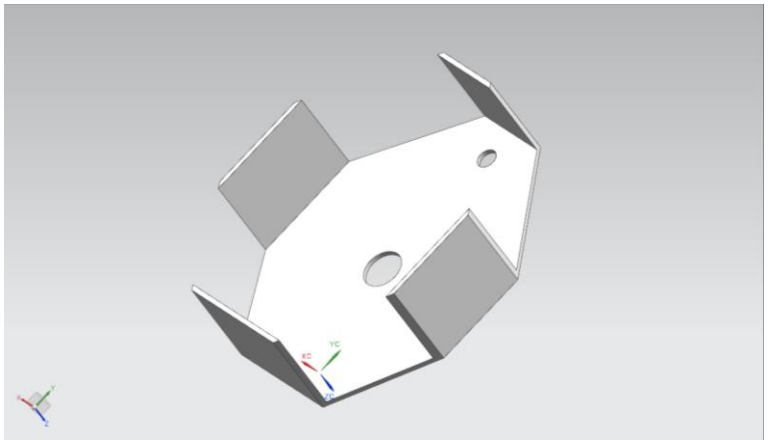

MC11. Final gearbox

Next, the gear mounts were designed to provide further supports for the gears. The dimensions for the gear mounts were extracted from the gears and gear box. Modeling process is shown in Figures MC12-14.

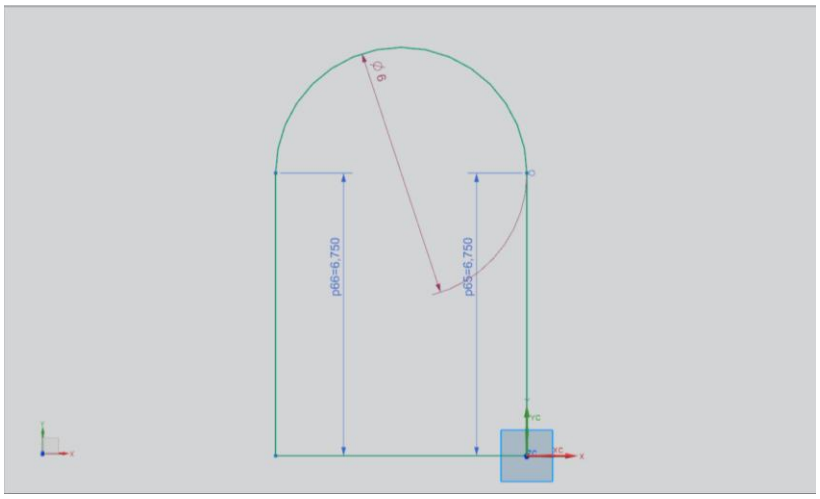

MC12. Sketch for large gear mount

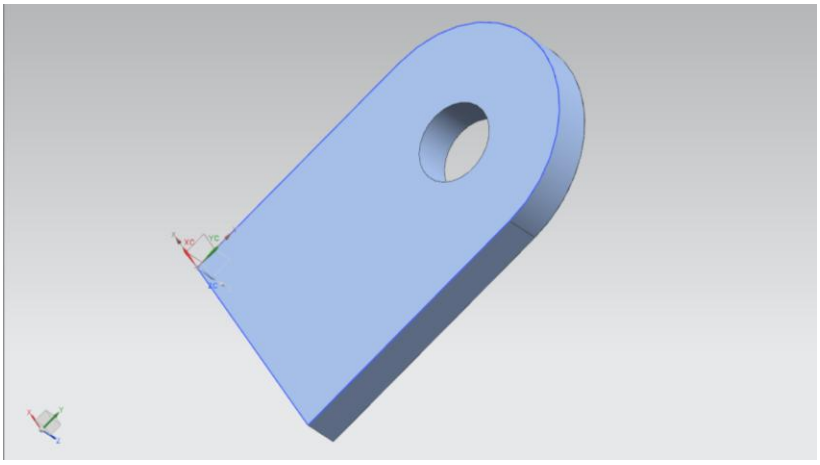

MC13. Extruded and Holed

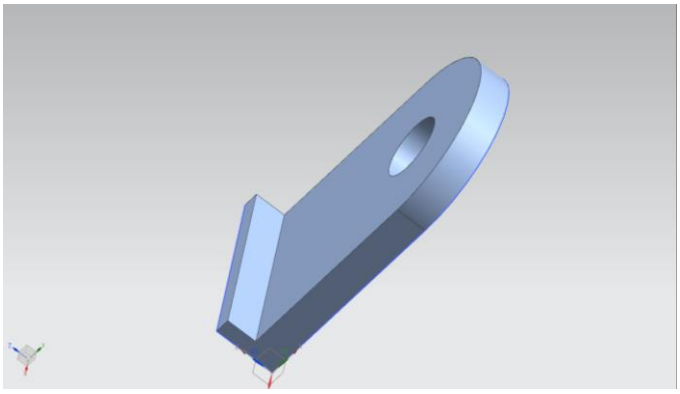

MC14. Attaching plate added using Extrude

Next, the smaller mount was modeled:

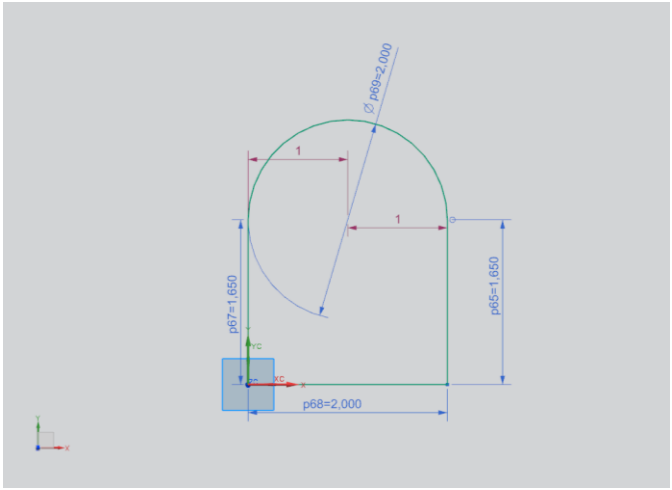

MC15. The sketch for the smaller gear mount

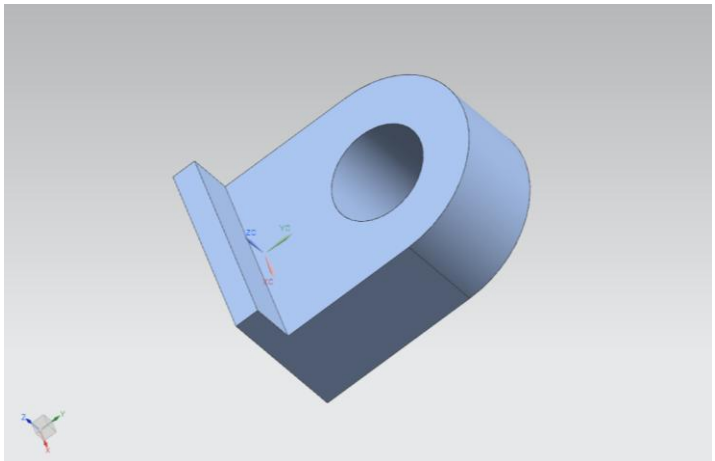

MC16. Completed smaller mount completed as the larger mount

Next, the parts were assembled into the gear box. First, the large gear mount was assembled by aligning the centerlines with respective hole and flushing it with the back of the gearbox. The same mount was assembled but it was flushed with the front face of the gearbox.

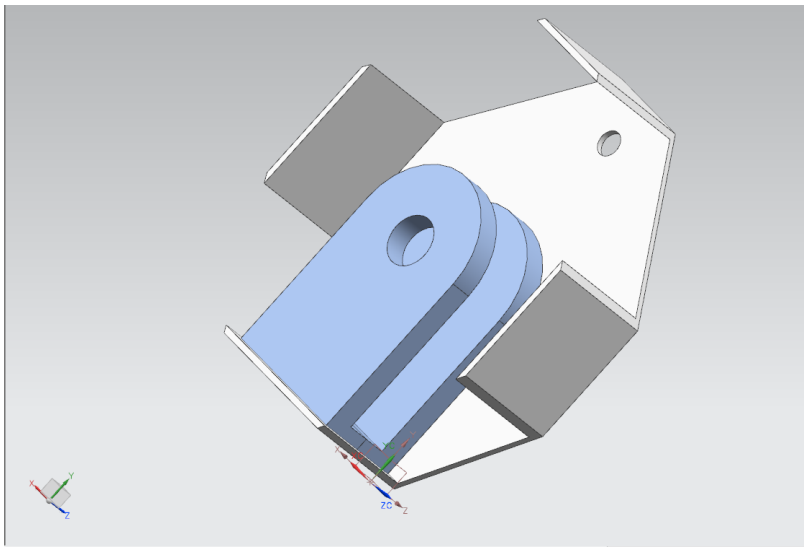

MC17. Extra support for heavier and larger gear

The larger gear was aligned with mount centerlines. It was then flushed and distanced from the faces of the mounts so that it runs in the middle to avoid friction.

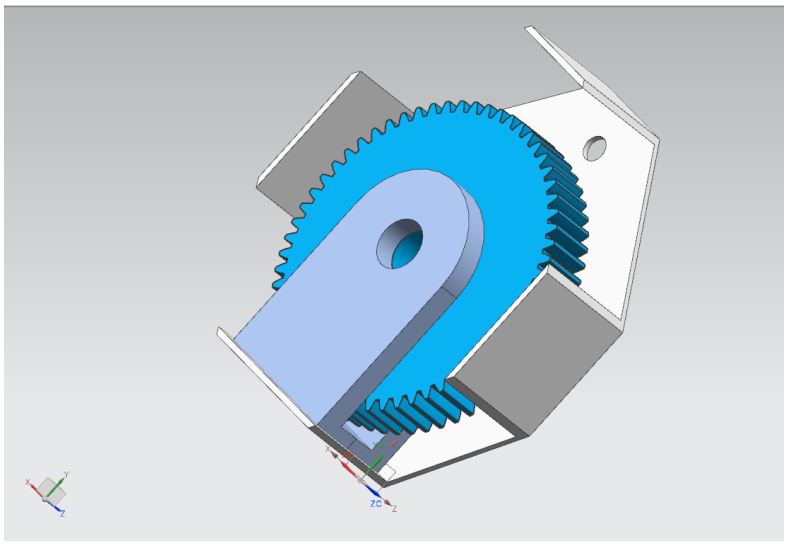

MC18. Large gear added

The smaller gear was assembled the same way and rotated so that the teeth line up.

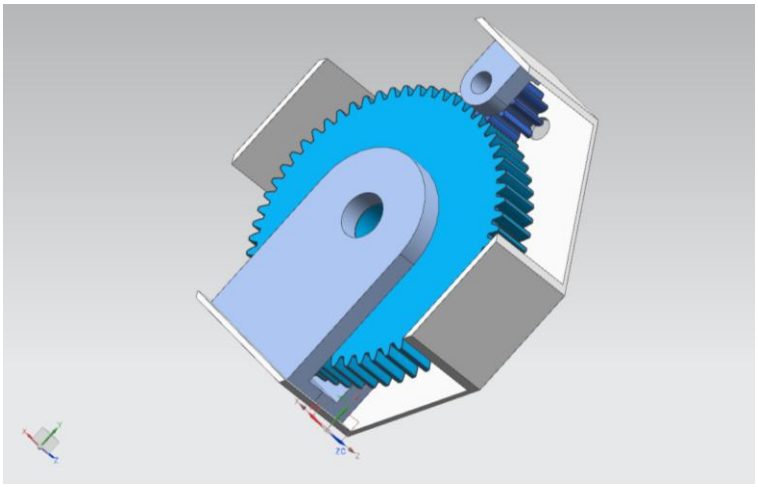

MC19. Both gears added and aligned

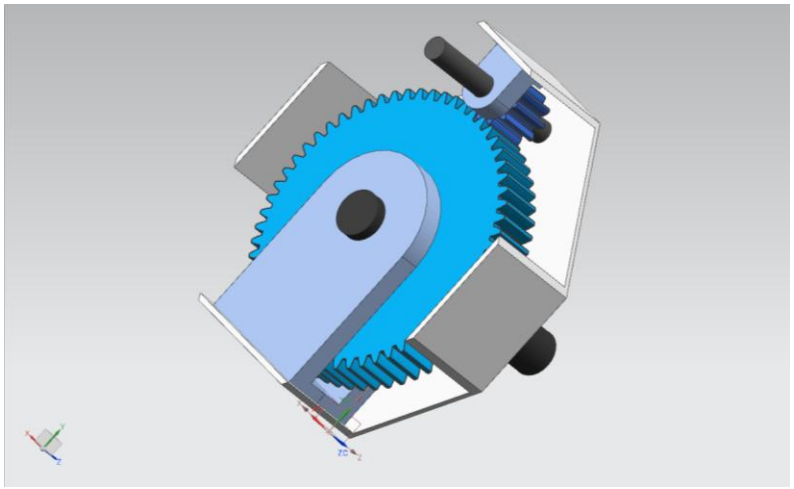

MC20. Final gearbox assembly with drive shafts added

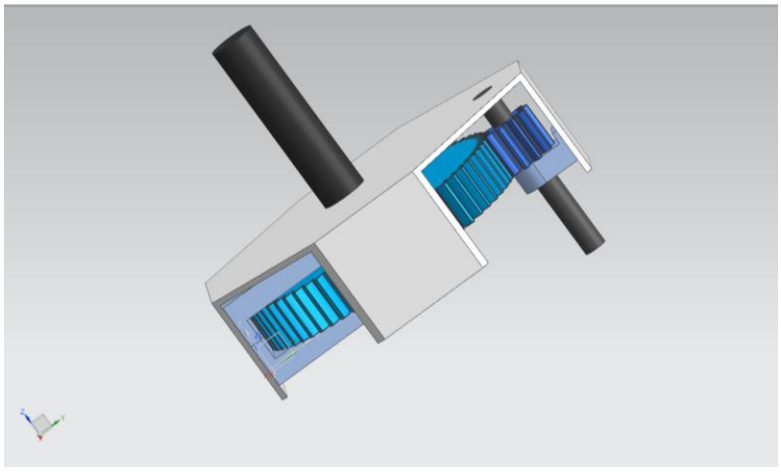

MC21. Final assembly of gearbox

Sprocket and Track Element Modeling

The driven wheel or sprocket was designed to be larger than idle wheels of the track system. This would increase the torque applied onto the tracks. Instead of using teeth on the sprocket, cavities were used to added complexity and aesthetic appeal. The modeling for the sprocket is illustrated in Figures MC22-24.

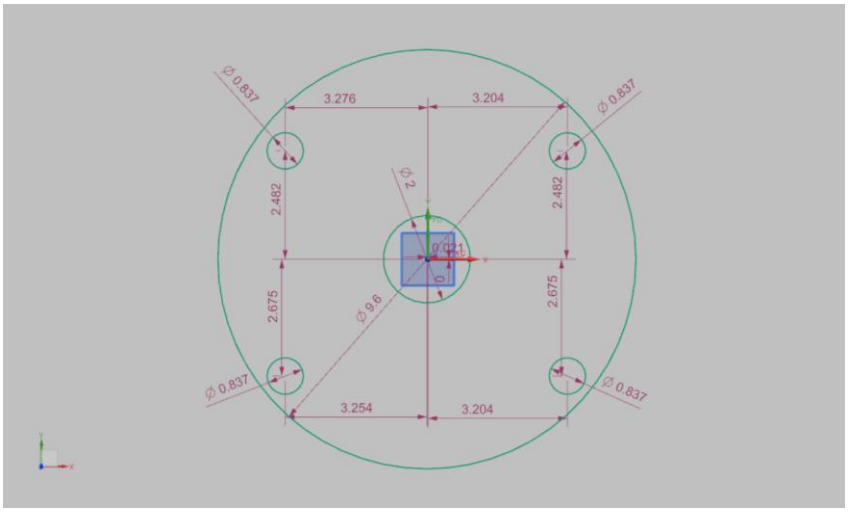

MC22. Sprocket sketch

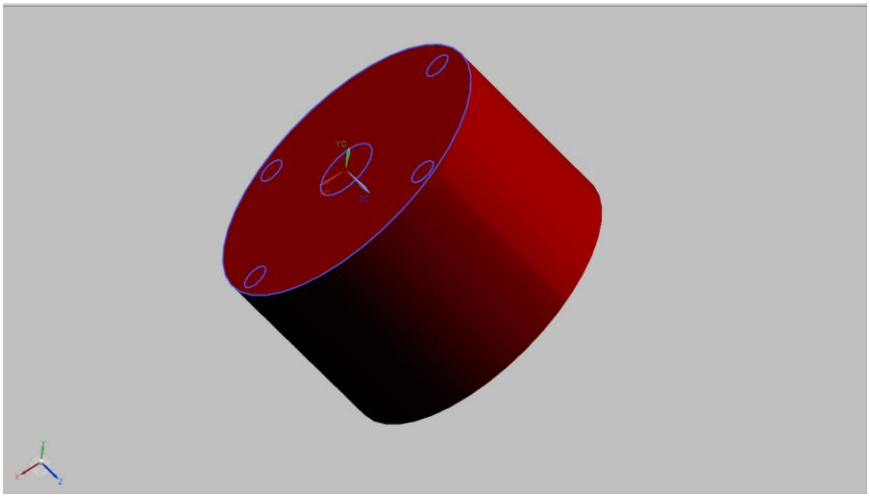

MC23. Extruded sketch

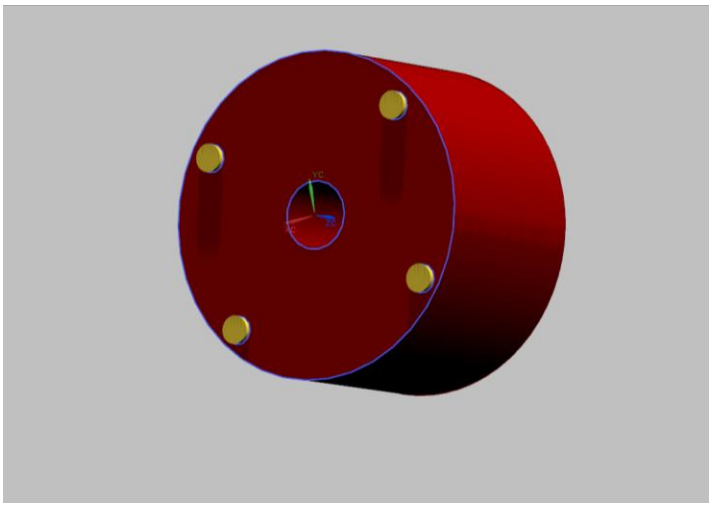

MC24. Sprocket with drive shaft hole but without driving cavities

Next, for the cavity, a profile was designed to avoid the belt shearing when torque is applied. The method of increasing cross section was applied to reduce the stress concentrations. The designed profile must also make it easy to remove and maintain the drive system. The belt is held in place using the tension applied by the idle wheels and sprocket. The profile for the cavity is shown in Figure MC25:

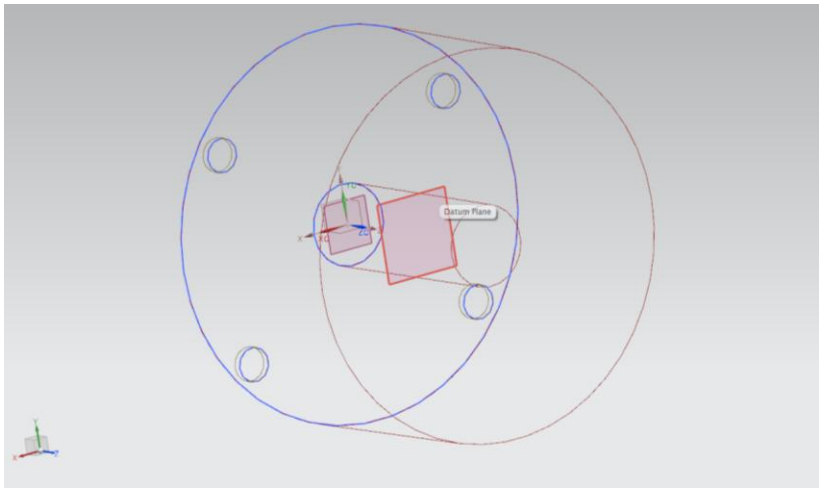

MC25. Datum plane in the middle of the wheel created

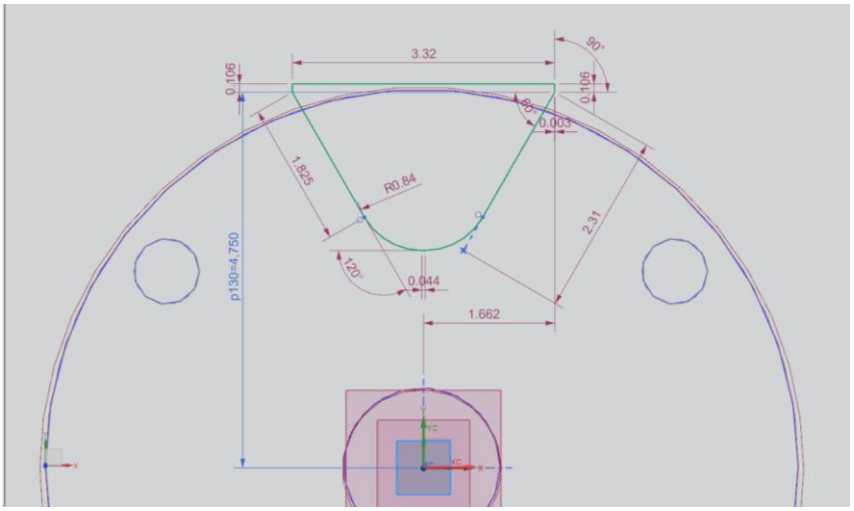

MC26. Driving cavity profile with increasing area

The cavity was created using extrusion subtraction and then patterned to have 8 cavities over 360 degrees.

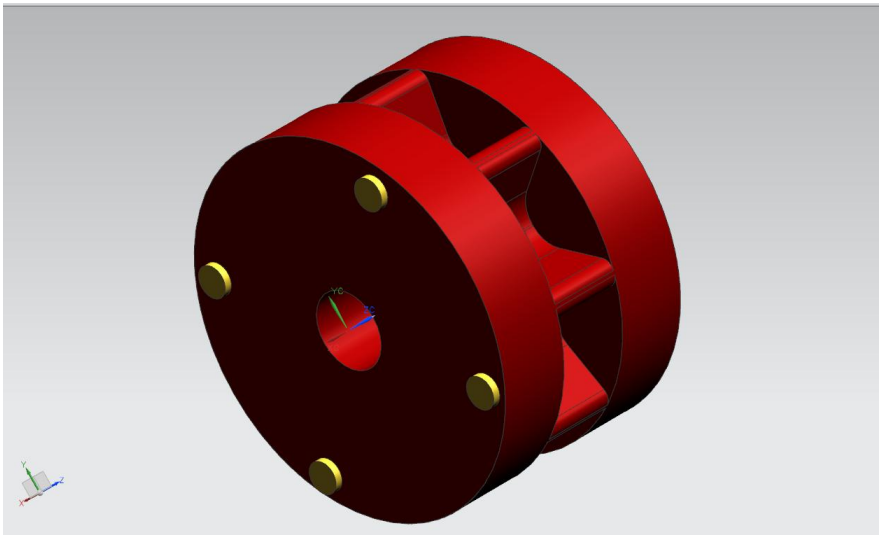

MC27. Finalized sprocket with edge blended cavities

Next, the track element was designed. The track element profile was selected to completely be incorporated in the sprocket and provide necessary traction to the robot. The track will be made of hardened polyurethane to be able to go around the track and has enough

coefficient of friction. The width of the track was selected to be 6 in. The profile for the track element is shown in Figures MC28-30:

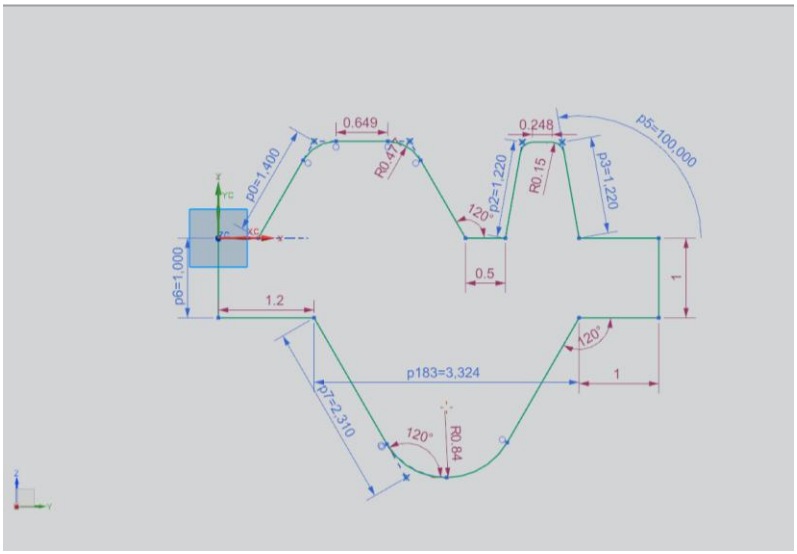

MC28. Track element profile

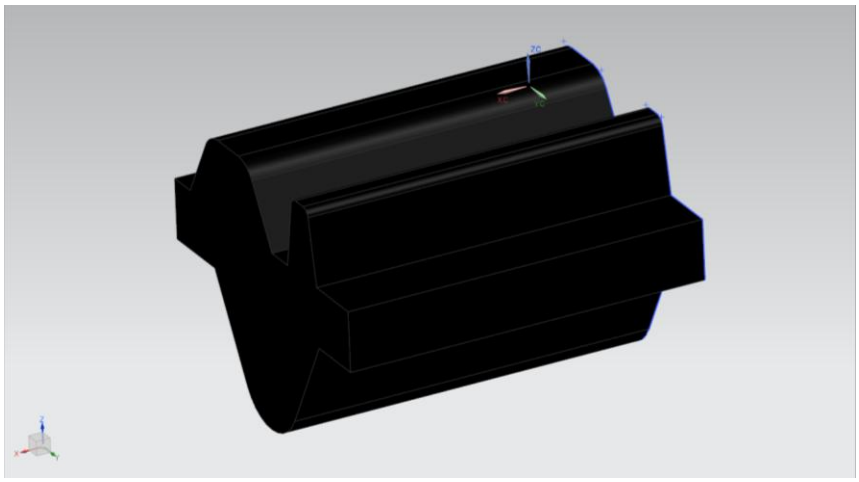

MC29. Extruded track element

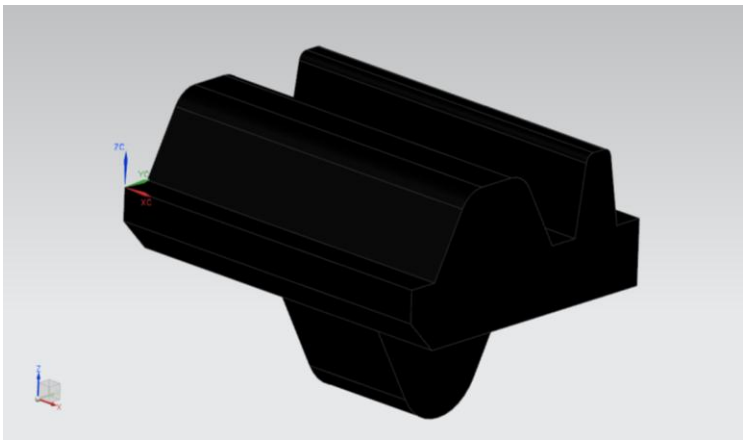

MC30. Final track element with correlation dimension with sprocket

Motor Modeling

The Perm PMG – 132 is geometrically complex motor and modeling it required a lot of datum planes, patterning and edge blends. The modeling illustrations are shown below:

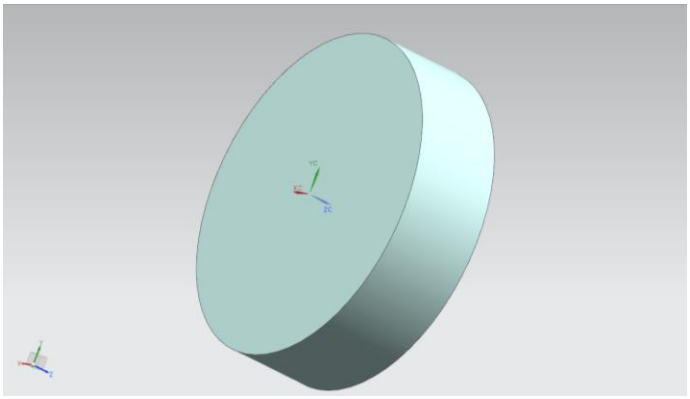

MC31. Basic extruded profile

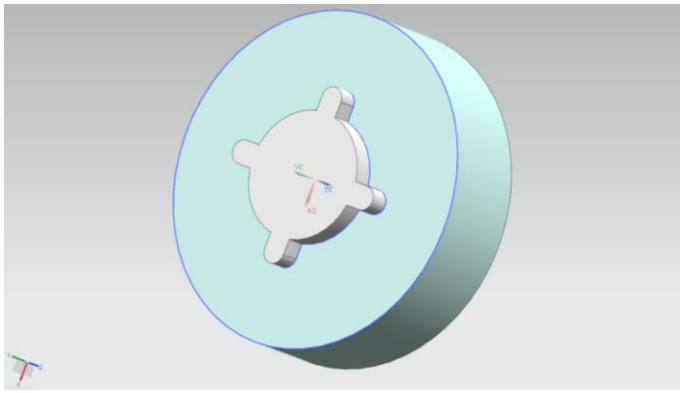

MC32. Spline was extruded to form the extrude

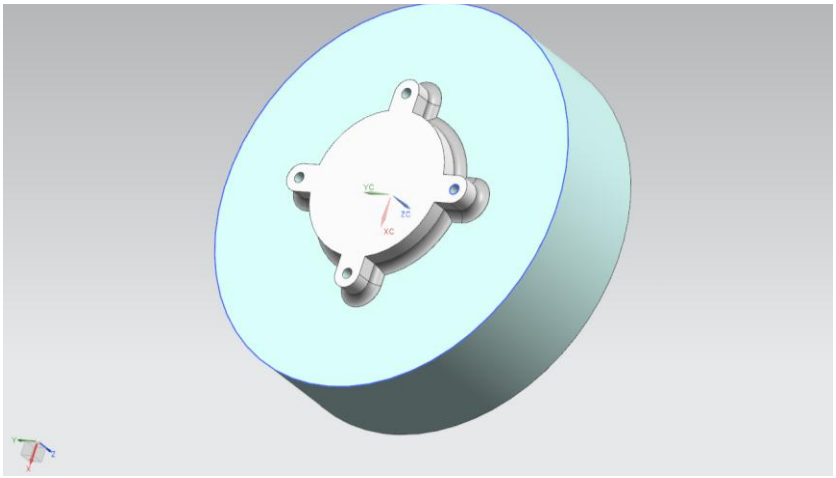

MC33. Edges blended and holes for drilled for bolts

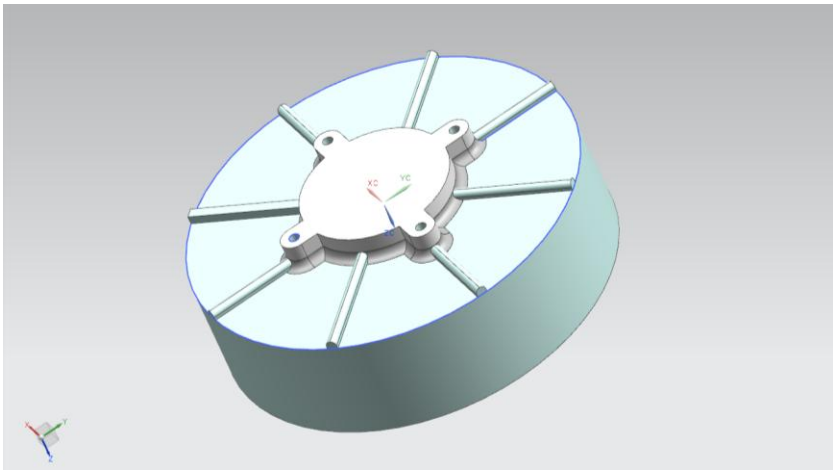

MC34. Profile extruded and edge blended

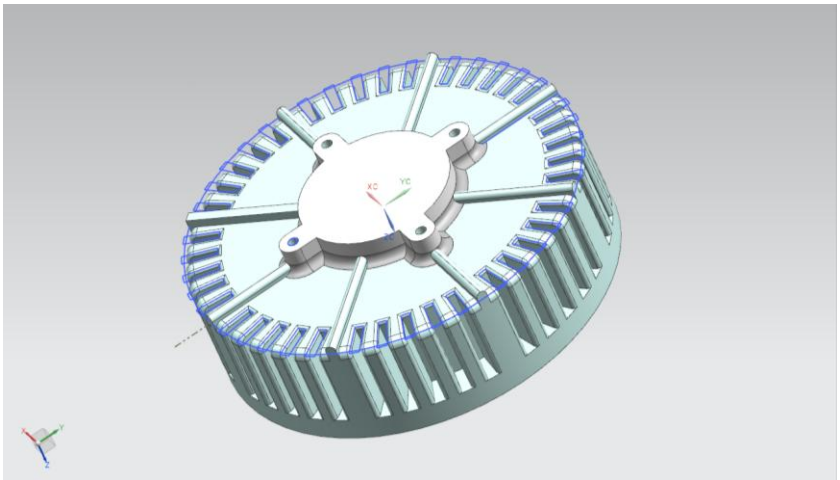

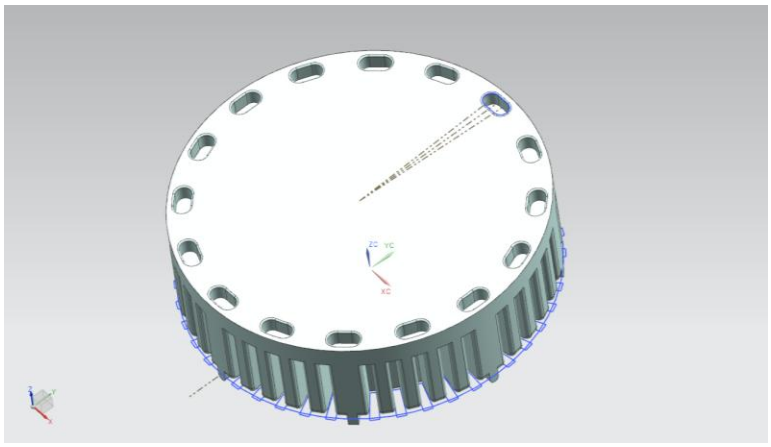

MC35. Extrusion subtraction, irregular patterning and edge blending to form the vents in the motor

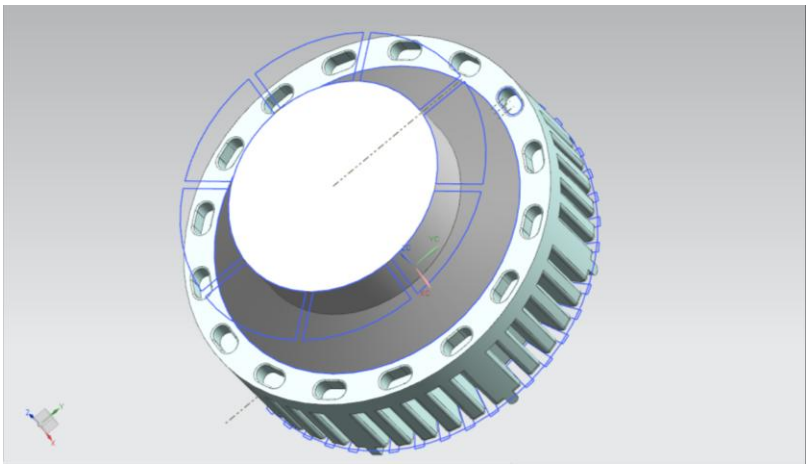

MC36. Forming struts using drafted extrusion and subtraction

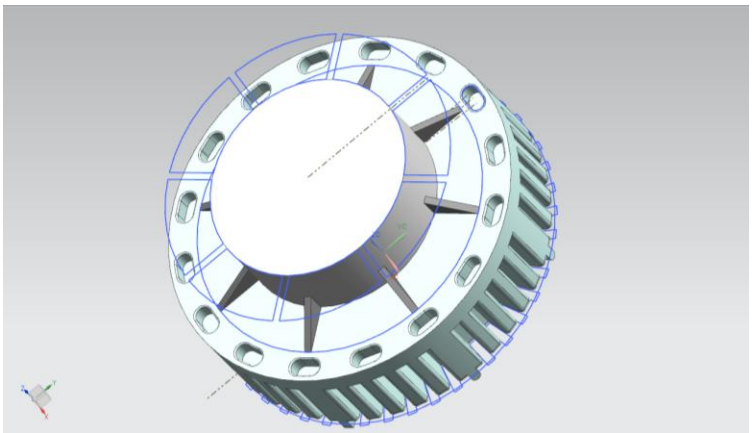

MC37. Struts formed

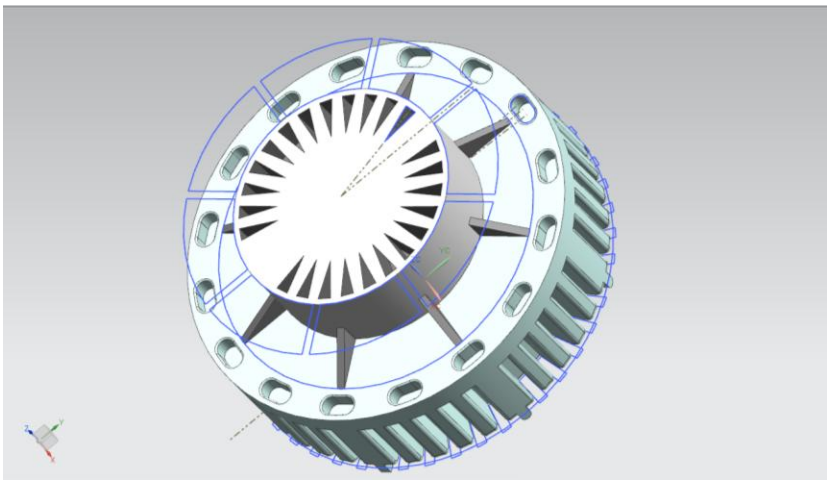

MC38. Additional vents formed using subtraction and patterning

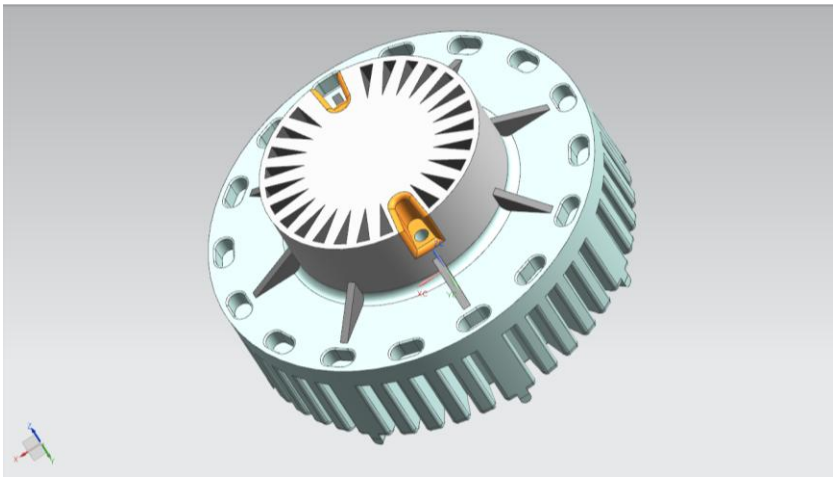

MC39. Final motor part with bolt holes at the back

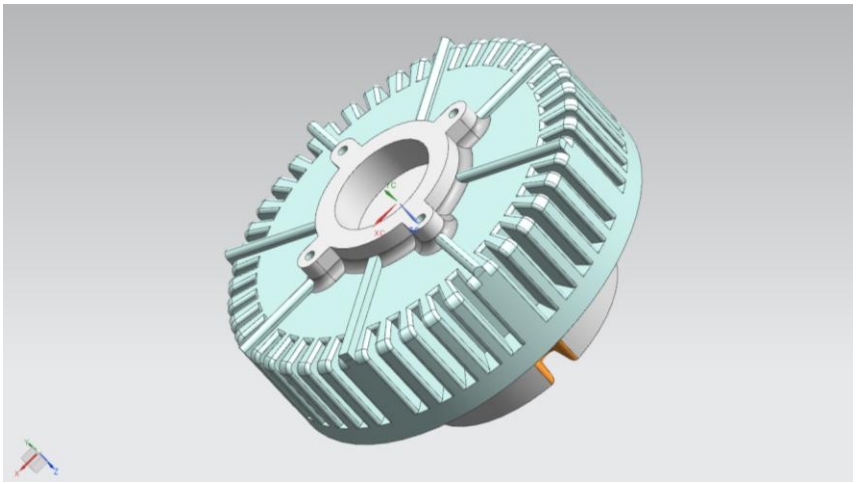

MC40. Front view of motor

Suspension Assembly

The suspension is an integral part of the system. It helps support the weight of the robot and also stops it from collapsing on itself. It also provides the much needed ground clearance that the robot desires. For the design the suspension was designed with a height adjustable apparatus. This helped to move the robot over some rough terrain that it might encounter during its task. The suspension assembly contains an upper connector, lower connecter, the spring, the air piston (for height adjustability), containment chamber for the air piston, a couple of bolts, an idle wheel connecting to it and a spurt that is attached to it, which in turn in connected to the wheel. Figure MD1 shows the final suspension assembly.

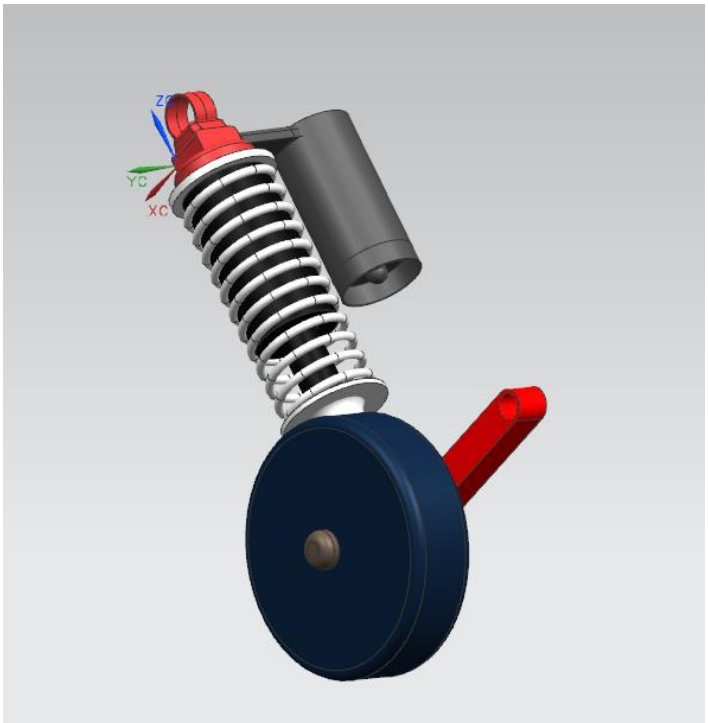

Figure MD1. Final Suspension Assembly

Spring Modeling

The spring modeling was done using the helical sketch option in NX 8.0. The diameter of the helical was determined to be 2.5 inches, the pitch was decided to be 0.5” and the number of

active turns that were given to it was 12. This helical sketch was used to give the spring its shape by using the tube function in NX 8.0. These results are shown in Figure MD2.

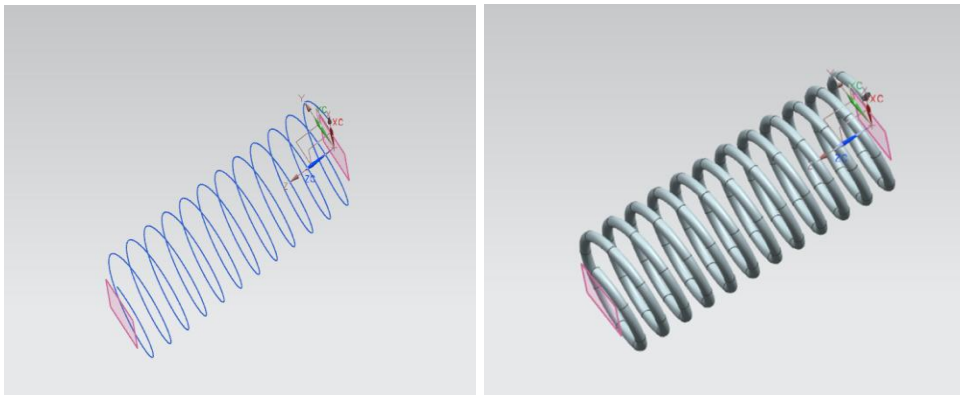

Figure MD2. Spring

The spring was constrained using two attachments on then top and bottom. To design these, datum planes were drawn at those respective locations and a circle was drawn and extruded. For the lower section though many other datum planes were drawn at small intervals and circles were drawn in decreasing diameter. After the completion of the respective circles, through curve function was used to give the lower section of the spring so that it follows a certain shape very similar to actual suspension systems. The results of these sketches are shown in Figure MD3 below.

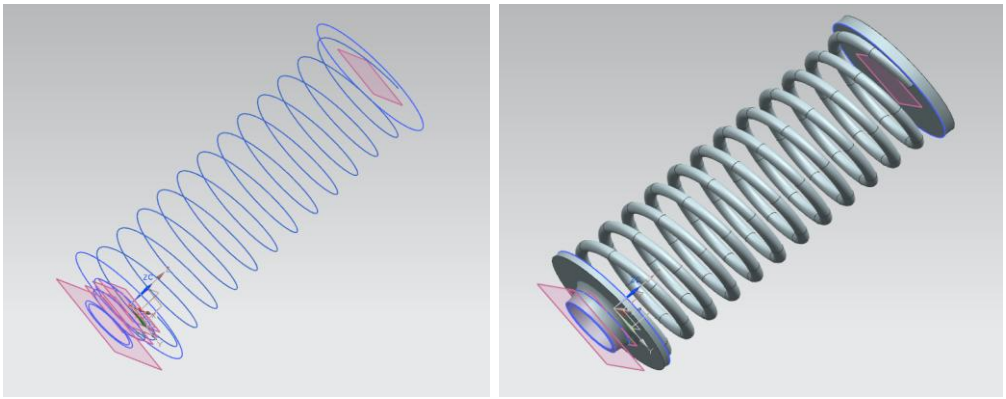

Figure MD3. Spring Constraints

Upper Connector Modeling

The purpose of the upper connector of the suspension system is to connect it to support the structure that will be shown later in this report. The upper connector was a relatively hard part to design as getting the dimensions for it with respect to the whole system was difficult. To sketch the upper system a couple of datum planes were used to create certain sketches at certain distances. These sketches were then extruded according to the respective dimensions. After the extrusions were done, then some smaller parts were subtracted to get the final effective shape of the upper connector. This resulted in a very boxy shape of the upper connector. To make it look more like a part of a suspension system, edge blends of diameter 0.15" were used to give it shape. The final results for this modeling process are shown in the Figure MD4.

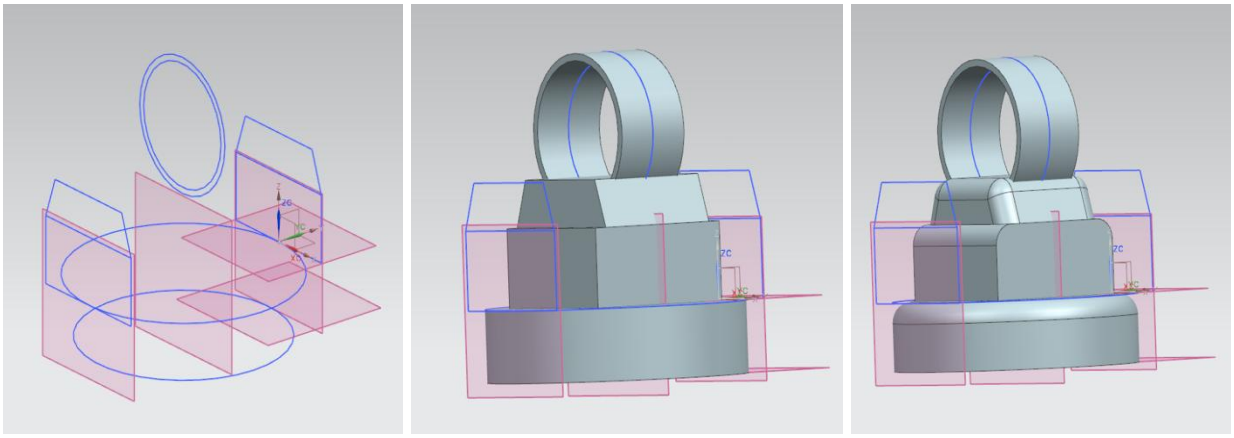

Figure MD4. Upper Connector

Lower Connector Modeling

The lower connector of the spring gets connected to the air piston which does the height adjustability of the robot. It is also attached to the wheel and the spurt in the final spring assembly. The design/sketching of the lower connector is very similar to the upper connector though the dimensioning of this part is different from the above mentioned part. This connector plays an important part in the assembly of the suspension system; hence the dimensioning has to

be spot. Because the design was from scratch, the dimension had to be hand calculated. For the design of the lower connector 2 datum planes were selected perpendicular to each other. This helped in sketching of the bolt holding hole and the base of the lower connecter. After this each sketch was extruded and subtracted according to the dimensions to get the respective shape. To make it look more like the actual suspension, a heavy use of edge blends was also done here. The final designs are shown in Figure MD5.

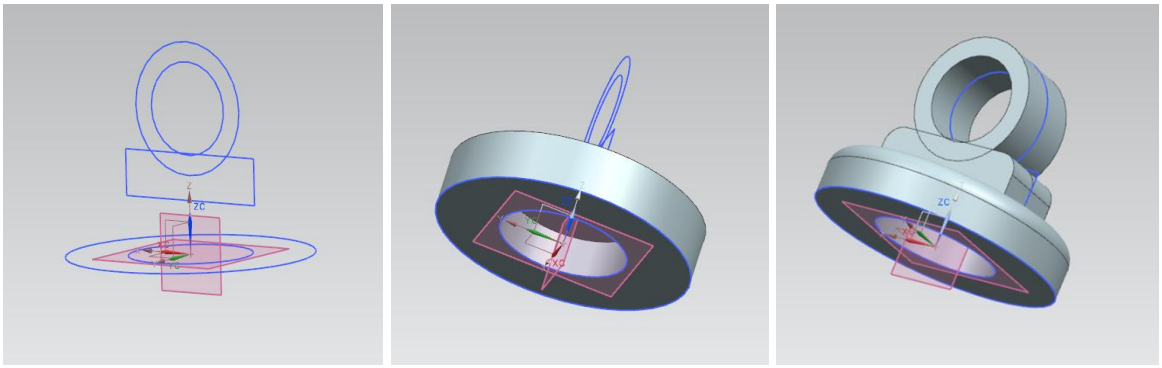

Figure MD5. Lower Connector

Air Piston Modeling

The air piston was one of the simpler design features of this project. It had basically 2 different sketches and 3 different extrusions. To start with a datum was selected to sketch on. On this datum plane a circle was sketched for the base of the air piston. This circle was extruded. Another circle was sketched at the datum plane and was extruded. This acted as the rod of the air piston. The result of these sketches is shown in Figure MD6.

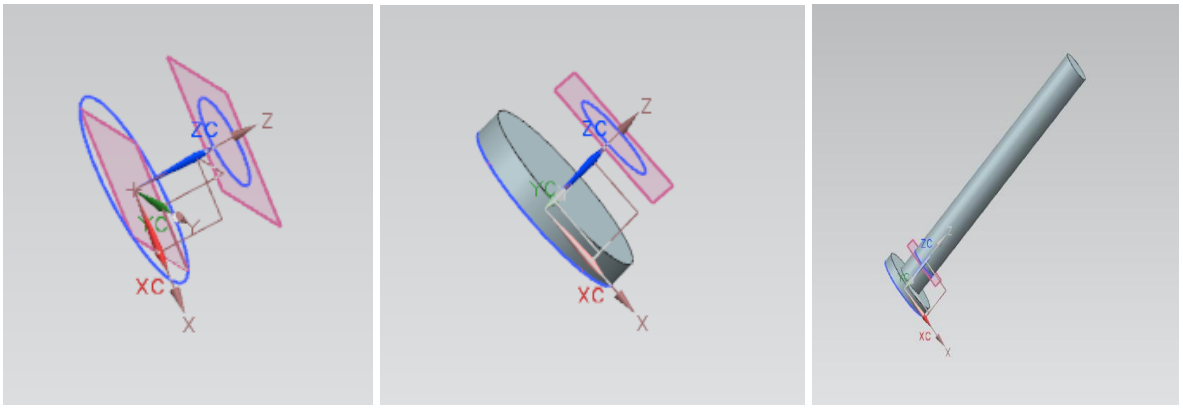

Figure MD6. Air Piston

Containment chamber for the air piston Modeling

The height adjusting apparatus has 2 parts within the spring suspension. The containment chamber contains the air pressure within it and the air piston and aides in the height adjustability of the robot. The containment chamber was designed using 3 main circular sketches and the use of extrusions and subtractions. During the sketching subtraction was used instead of the shelling feature as the making minute changes to the dimensions are easier when simple extrusions are used. The final design sketches are shown in Figure MD7.

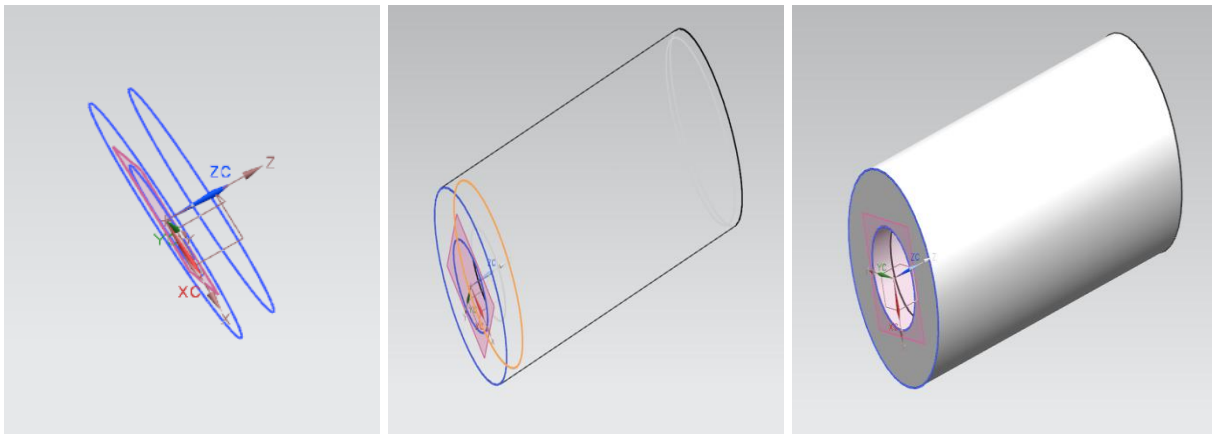

Figure MD7. Containment Chamber

Once both the designs for the air piston and containment chamber were done, they were assembled together in the assembly file to create the height adjusting apparatus. The final assembly of the height adjustability apparatus is shown in Figure MD8.

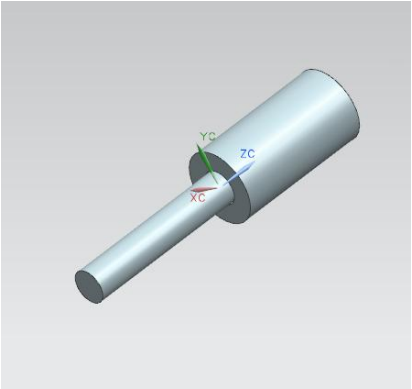

Figure MD8. Height Adjustability Apparatus

Suspension Assembly Modeling

After the completion of the design of the different components of the suspension, the components were assembled in an assembly file. The height adjusting apparatus was constrained with in the spring but the air piston was free to move up and down in the containment chamber. The upper connector was constrained to the upper section of the spring and its rotational motion was also constrained. The lower connector was constrained to the air piston and its rotational motion was also constrained. All these resulted in the final assembly of the spring suspension as shown in Figure MD9.

Figure MD9. Suspension Assembly

Gas Compressor Modeling

For the air piston to work, it needs to be delivered with gas. This in turn will push it and it will generate height difference for the robot. For the design of the air compressor 2 datum planes perpendicular to each other were used. On these the sketches of circles and a rectangle were drawn. These sketches were extruded respectively and edge blended to give the final shape of the component. The rectangular extrusion was the place from where the gas for the working of the air piston was delivered. The final sketches/design for the gas compressor is shown in the Figure MD10.

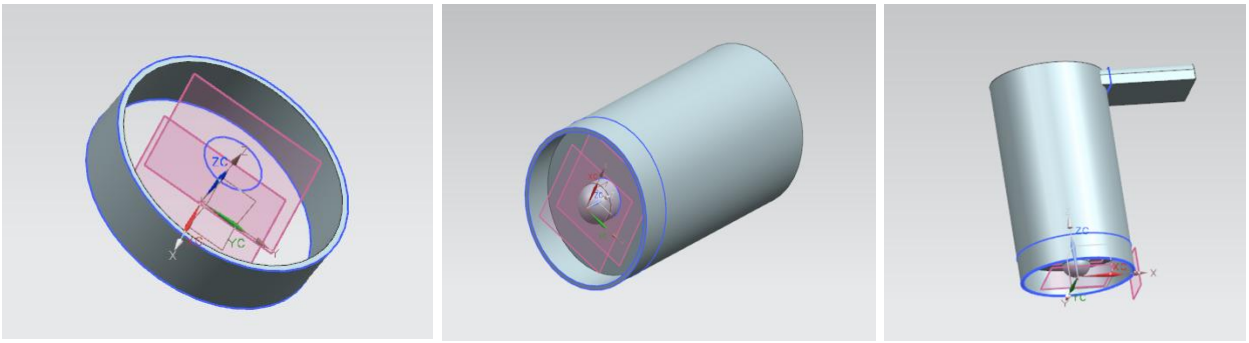

Figure MD10. Gas Compressor

Spurt Modeling

For the pivotal motion of the suspension, a spurt had to be designed. The spurt as acts as the connection between the rigid suspension and the wheel. The pivotal movement of the spurt helps in the height adjustability of the robot. The spurt has a simple design. It has two holes from where it can be connected to support structure and the wheel/suspension. The two holes are connected to each other using a line. The second hole also has a section where the lower connector of the suspension can be connected to spurt and the wheel together using a bolt. The various design features and the final design is shown in Figure MD11.

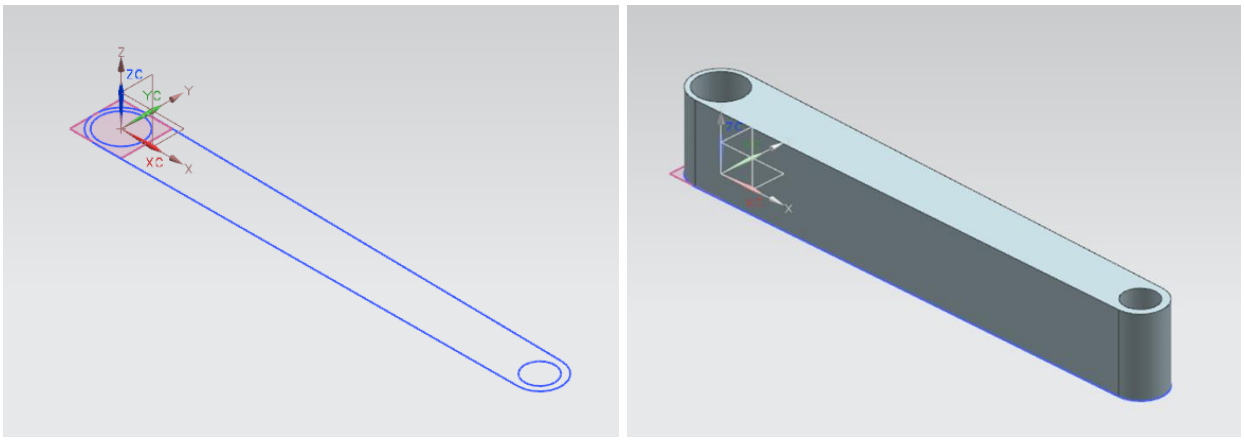

Figure MD11. Spurt

Idle Wheel Modeling

The robot has 7 wheels on each side. One of the wheels is the sprocket that is driven using the motor. The other 6 wheels are “idle” but they are in tension within the tracks. Two of the wheels are right next to each other and have a gap of 2”. This is where the suspension and the spurt of the wheels are inserted. The spurt, the wheel and the suspension are held together using a simple bolt. The sketch of the wheel consisted of 2 circles and then extruded. The second circle (smaller one) acts as the hole for the bolt to be inserted in. The final sketches and the design are shown in Figure MD12.

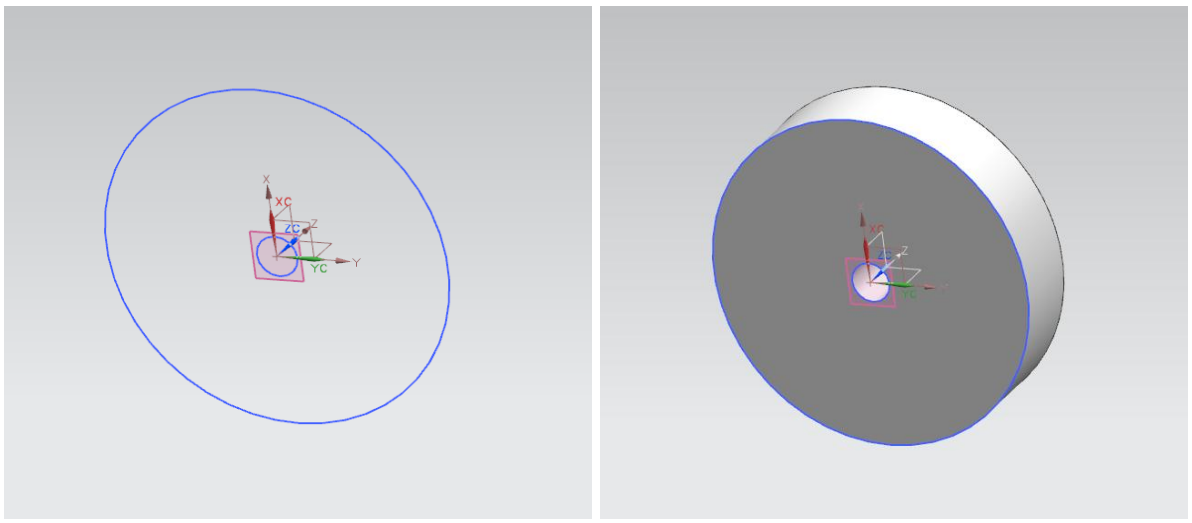

Figure MD12. Idle Wheel

Bolt Modeling

Bolt is one of the most integral and important of the suspension system. It connects all the different components to give the final suspension assembly. For this robot, a general shape of the bolt was designed. Then it was changed according to the different dimensions required for the different holes that it was to be inserted through. The bolt had a simple sketch of two circles. Each of these sketches was extruded according to the respective dimensions. Edge blend was used to make the head of the bolt more curved. The final sketches and the design are shown in Figure MD13.

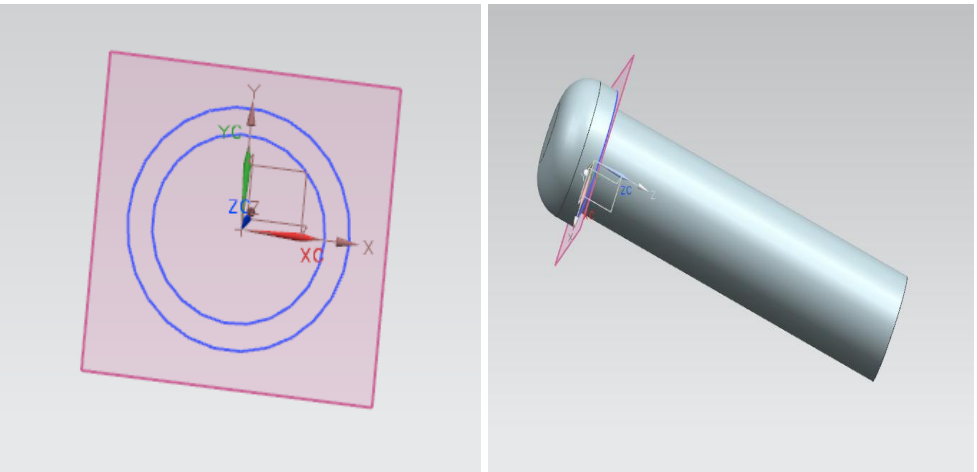

Figure MD13. Bolt

Support Structure Modeling

The support structure gives the much needed stability to the suspension structure. This is where the spurt and the suspension assembly are attached and then they are attached to the wheel. The support structure helps in supporting the weight of the robot. The support structure sketched in more datum plane. This was due to the fact that it was one long structure. The holes were made in the support structure keeping in the mind the overall dimensions of the robot, the spurt and the suspension assembly. The sketch was then extruded to get the final result. The final sketches and the design for the support structure are in shown in Figure MD14.

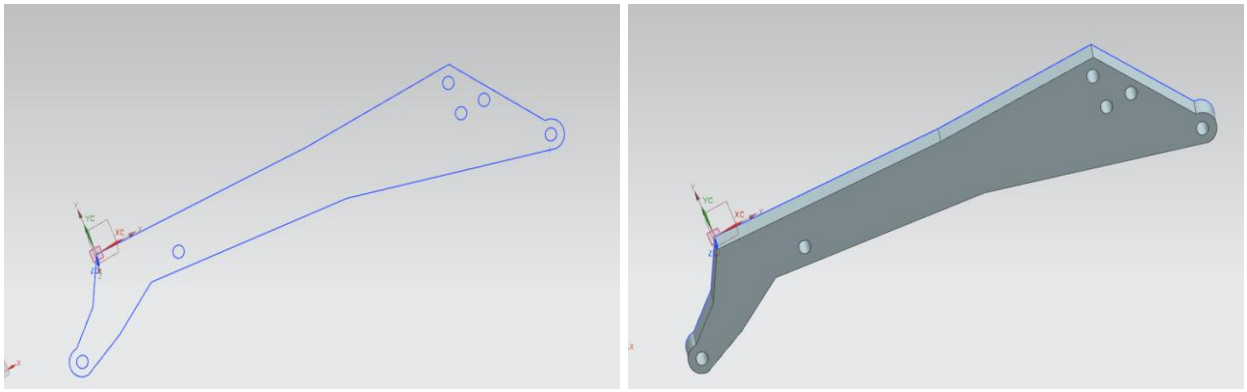

Figure MD14. Support Structure

Final Suspension Assemblies

Once all the components had been respectively modeled, they were assembled together using the various constraints that were need. The final two assemblies are shown in Figures MD15 and MD16 respectively.

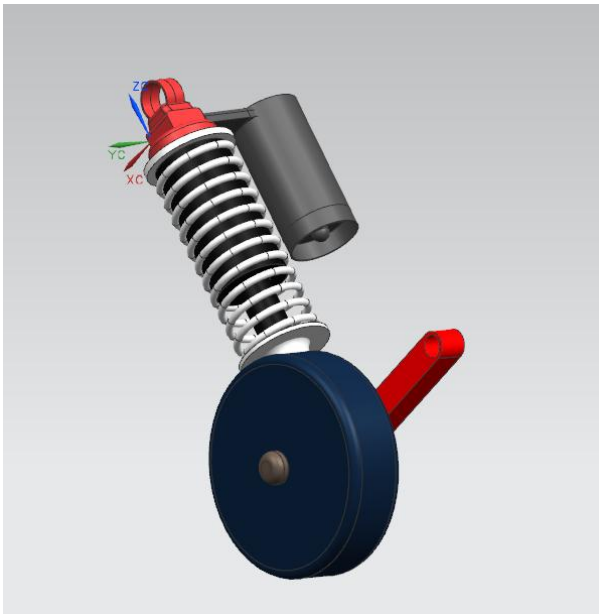

Figure MD15. Without Support Structure

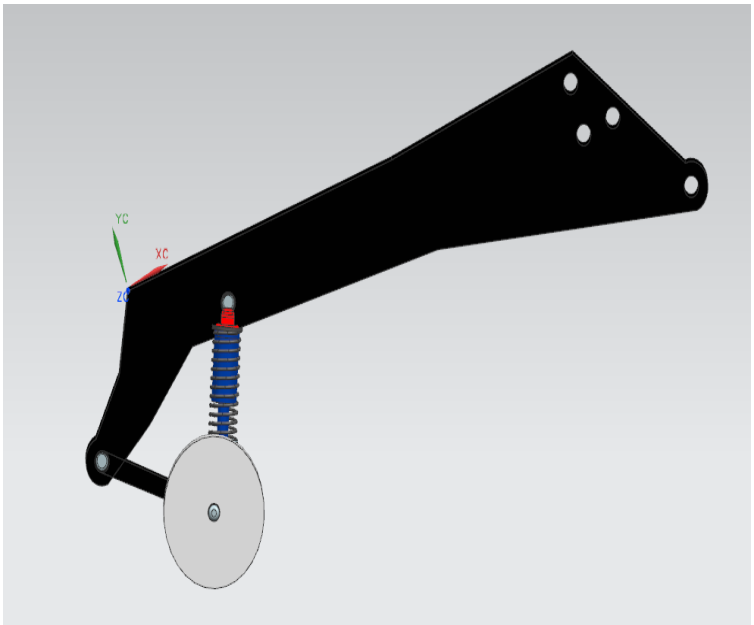

Figure MD16. With Support Structure

Final Robot Assembly

The final robot assembly is depicted in Figure ME1. It consists of the infrared camera, insulated frame, electronics cooling system, drive system, and suspension system.

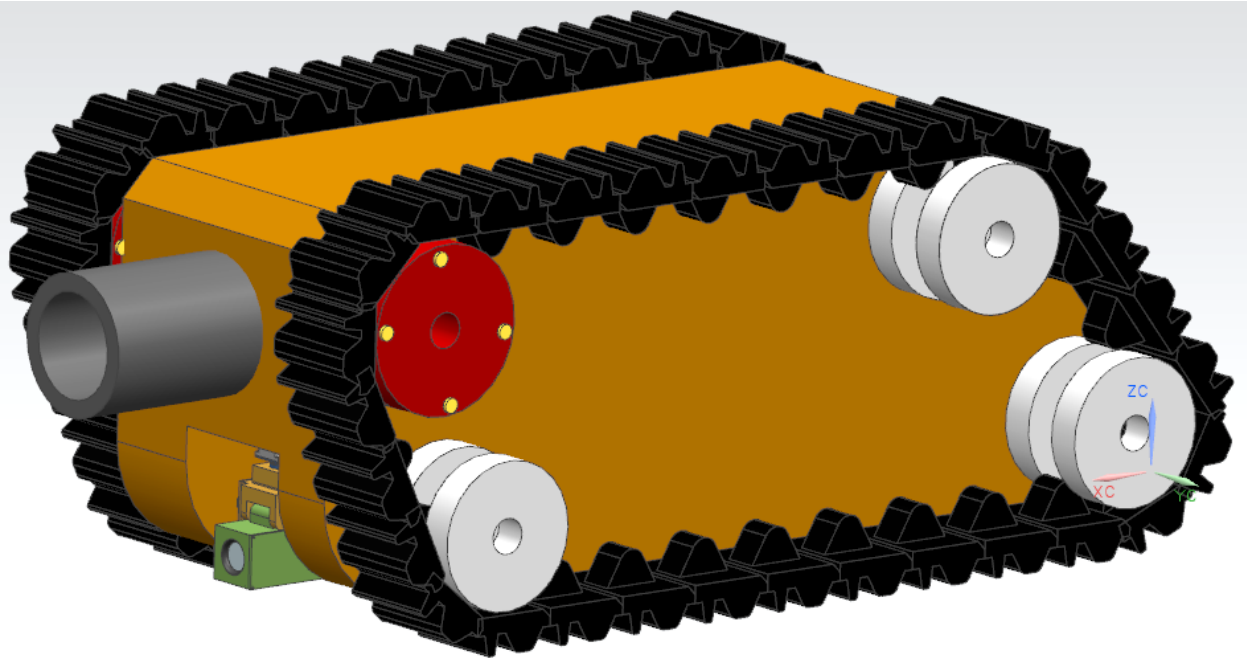

Figure ME1. Robot Assembly

ANALYSIS

Problem 1: Linear Spring System

One of the main components for maintaining the stability of the robot is the suspension system. It had to be simple in design and should fit the design constraints set by the robot. In the design, taking the space limitations into consideration, it was decided that a 6 inch length, 2.2 inch outer diameter, and 12 coils spring with a pitch of 0.5 inch would be used. The weight of the robot (120 kg) would be equally distributed among four individual suspension systems. Thus, each spring will feel a 300 N force. The spring is shown in Figure A1.

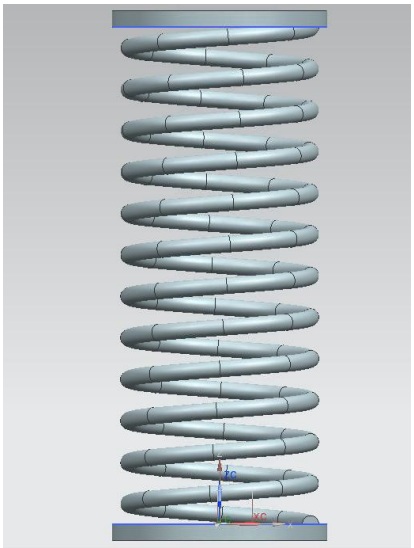

Figure A1. Basic Spring Structure

Hand Calculations

A basic setup of the spring system is shown in Figure A2.

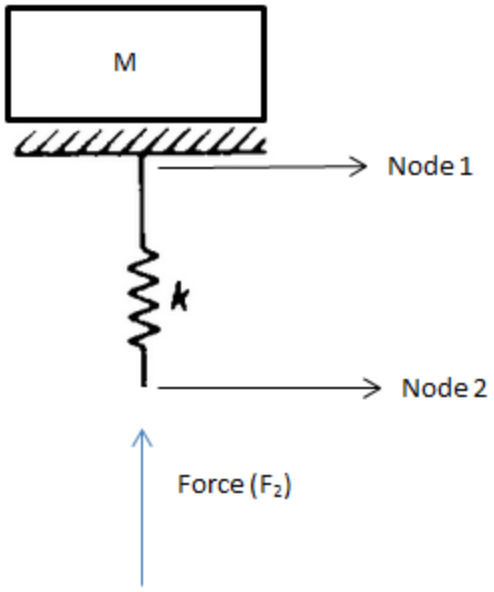

Figure A2. Spring System Sketch

In this setup the spring has only two nodes; one is constrained. Since the spring is linear, the force exerted by the mass is equal and opposite to F_2. The force exerted by every single mass is 300 N. Node 1 is constrained to have no deflection. For this design the max deflection has to be calculated. Since the dimensions of the spring and the material (Steel) are known, the spring constant *k* for the spring in question was calculated using Equation A1

$$k = \frac{Gd^4}{8nD^3} \tag{A1}$$

where *G* is the shear modulus, *d* is the diameter of the spring wire, *D* is the outer diameter of the spring, and *n* is the number of active coils. Plugging G = 79.3 GPa [1], d = 0.1 in, n = 12 and D = 2.2 in, the spring constant was determined to be 7757.71 N/m.

Using a single matrix equation as shown in Equation A2, the maximum displacement for the spring was determined.

$$\begin{Bmatrix} f_{1x} \\ f_{2x} \end{Bmatrix} = \begin{bmatrix} k & -k \\ -k & k \end{bmatrix} \begin{Bmatrix} d_{1x} \\ d_{2x} \end{Bmatrix} \tag{A2}$$

where the forces, f_{1x} and f_{2x} (300 N) are equal and opposite. Displacement d_{2x} needs to be determined while $d_{1x} = 0$. This can be determined using

$$f_{2x} = k(d_{2x} - d_{1x}) \tag{A3}$$

The maximum displacement was calculated to be 1.517 in.

Computer FEA using NX

To perform the calculations for displacement using the computer, the NX 8.0 Advance simulation package was run. The spring had undergone structural analysis in this simulation to determine the maximum displacement it could achieve. The spring was assigned the steel material to match the hand calculations. The top section of the spring was constrained fixed, while a force was applied vertically at the bottom. A mesh size of 0.1 was used. Once the analysis was run, the resultant maximum displacement that the spring could sustain was 2.015 in. These results are depicted in Figures A3 and A4.

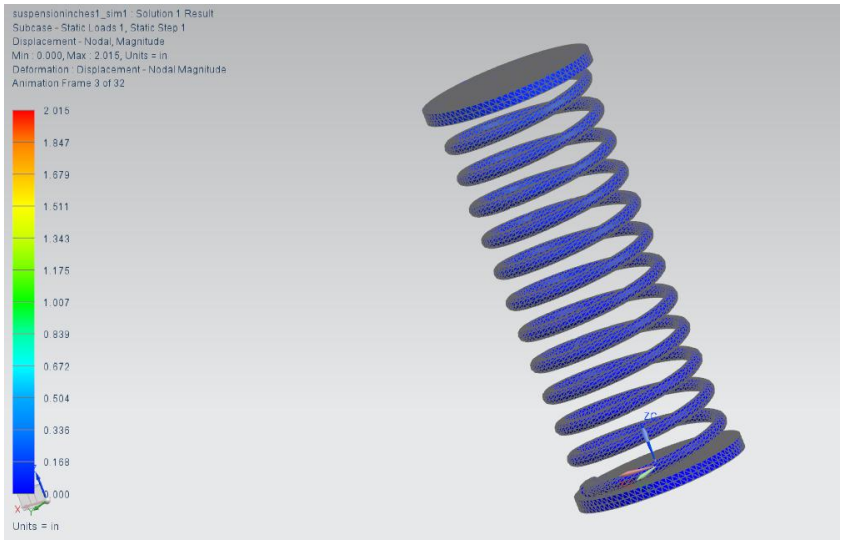

Figure A3. NX Analysis Initial State

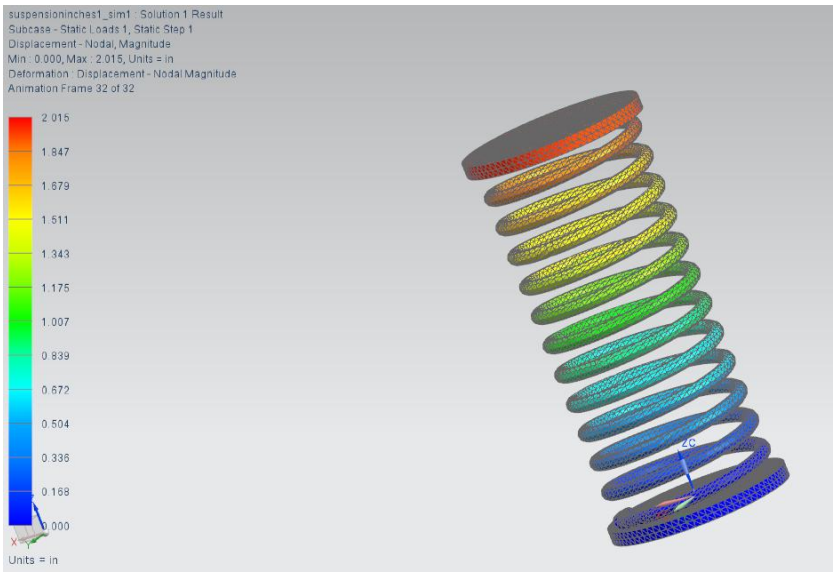

Figure A4. NX Analysis Final State

The computer calculation of 2.015 in. is 33% greater than the hand calculated displacement of 1.517 in. This may be due to the fact that NX 8.0 does nodal analysis. Also, NX distributes the load across all selected nodes. Hand calculations were an overly simplified version of the calculations, and hence, were not as accurate as desired.

Problem 2: Heat Sink Cooling

The electronics in the robot are cooled using fins. A one-dimensional conduction with convection analysis is carried out on the fins. The heat generated from the electronics is conducted to the fins, which loses the heat to water flowing over them through convection. A steady state is obtained over time, which keeps the temperature of the electronics at a constant 40°C.

Hand Calculations

The following sketch depicts the heat transfer problem.

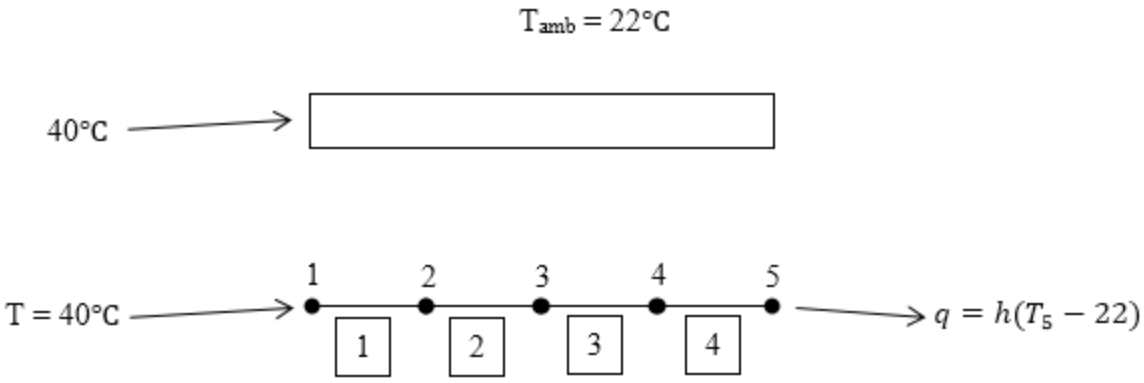

Figure A5. Fin Sketch showing the boundary conditions

The fins are made of aluminum. The fin diameter (D) is 0.0127 m, length (L) is 0.1016 m, the heat conduction coefficient (k_x) is 208 W/m-°C [2], the heat convective coefficient of water (h_{water}) is 568 W/m^2-°C [3], ambient temperature of water (T_a) is 22°C. A finite element solution for the temperature distribution across the length of the fin is carried out using four equal-length, two-node elements. The boundary conditions used are as follows,

At node 1: $$T_1 = 40°C$$

At node 5: $$q_5 = h(T_5 - 22)$$

The length of each element (L_e) was computed to be 0.0254 m, peripheral dimension of the differential element (P) was calculated as 0.0399 m, and the area (A) as 0.00013 m^2. The conductance matrix used is

$$k^e = \frac{k_x A}{L}\begin{matrix}1 & -1\\ -1 & 1\end{matrix} + \frac{hPL}{6}\begin{matrix}2 & 1\\ 1 & 2\end{matrix} \quad \text{(A4)}$$

After substituting values of the variables, the conductance matrix was obtained as

$$k^e = \begin{matrix}1.257 & -0.969\\ -0.969 & 1.257\end{matrix}$$

Following the direct assembly process, the system conductance matrix is as

$$K = \begin{matrix} 1.257 & -0.969 & 0 & 0 & 0 \\ -0.969 & 2.514 & -0.969 & 0 & 0 \\ 0 & -0.969 & 2.514 & -0.969 & 0 \\ 0 & 0 & -0.969 & 2.514 & -0.969 \\ 0 & 0 & 0 & -0.969 & 1.257 \end{matrix}$$

The convection force components per element was calculated using

$$f_h^{(e)} = \frac{hPT_aL}{2} \begin{matrix} 1 \\ 1 \end{matrix} \quad \text{(A5)}$$

Assembling the contributions of each element at the nodes, the system convection force vector is

$$F_h = \begin{matrix} 6.332 \\ 12.664 \\ 12.664 \\ 12.664 \\ 6.332 \end{matrix}$$

Similarly, the system gradient vector is calculated to be

$$F_g = \begin{matrix} Aq_1 \\ 0 \\ 0 \\ 0 \\ -0.074T_5 + 1.624 \end{matrix}$$

The finite element form to compute the temperatures is

$$K\ T = F_h + F_g \quad \text{(A6)}$$

Solving by Gaussian elimination, the nodal temperatures were obtained as follows

$$\begin{matrix} T_2 \\ T_3 \\ T_4 \\ T_5 \end{matrix} = \begin{matrix} 32.53 \\ 29.14 \\ 27.21 \\ 24.60 \end{matrix} \ ^\circ\text{C}$$

Computer FEA using NX

To perform the calculations for temperature distribution, the NX 8.0 Advance simulation package was used. Thermal analysis was carried out on the fin to determine the temperature distribution. All assumptions for the fin were matched with the hand calculations assumptions.

Two boundary conditions were used: temperature at one end was fixed at 40℃ to match the desired temperature, and a heat flux value of ~110,000 W/m^2 was used, which was computed as a result of the heat transfer analysis. The results are depicted in Figure A6.

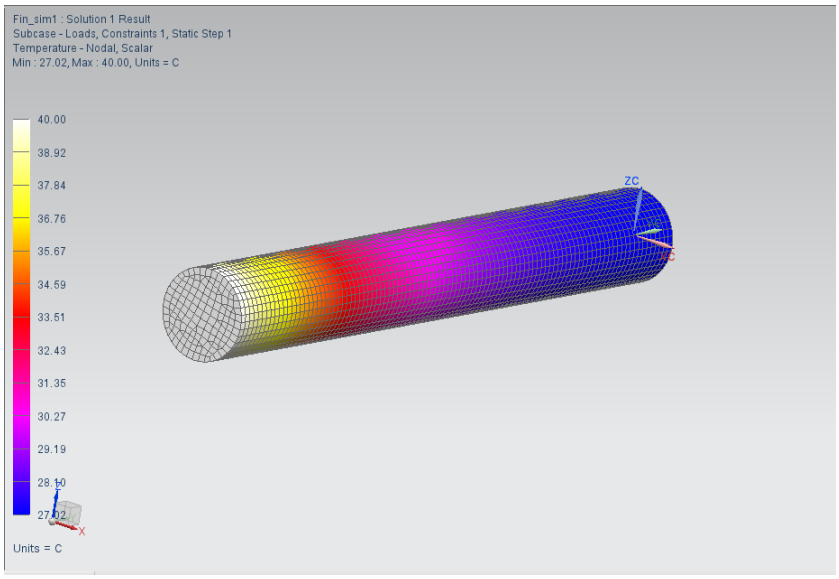

Figure A6. NX Results for Temperature Distribution

The maximum and minimum temperatures obtained were 40℃ and 27.02℃, respectively. The temperature gradient obtained is in agreement with the hand calculations. However, the minimum temperature obtained from FEA analysis is different from the one obtained from hand calculations. This discrepancy arises from the fact that FEA computes and performs analysis at each node, whereas hand calculations used only a small number of nodes. Thus, the FEA results are deemed more accurate.

Problem 3: Support Structure

The support structure was used in the drive system to connect the wheels to the sprocket and keep them intact. Figure A7 shows the geometry of the support structure part.

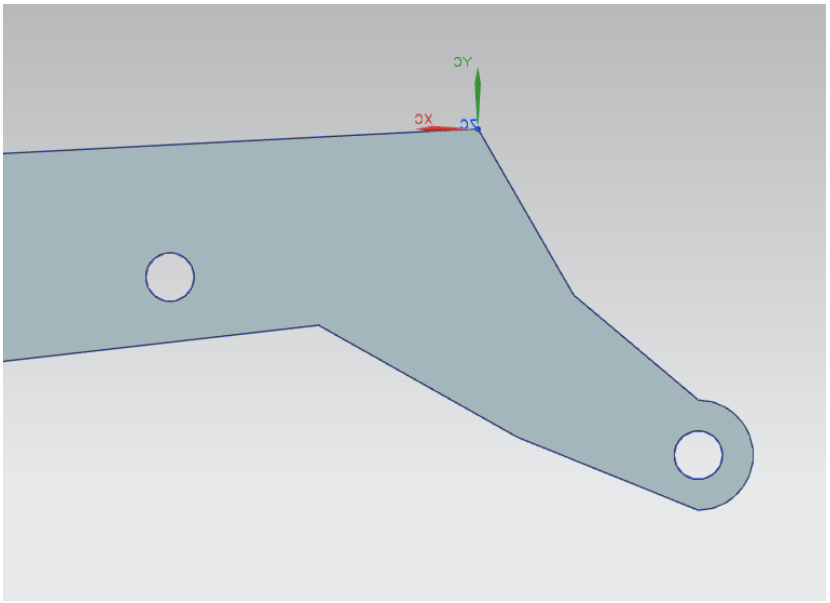

Figure A7. Support Structure Geometry

The geometry is complicated for hand calculations and sufficient guesses about the maximum deflection of the part can be made by simplifying it.

Hand Calculations

The simplified geometry is displayed in the sketch below.

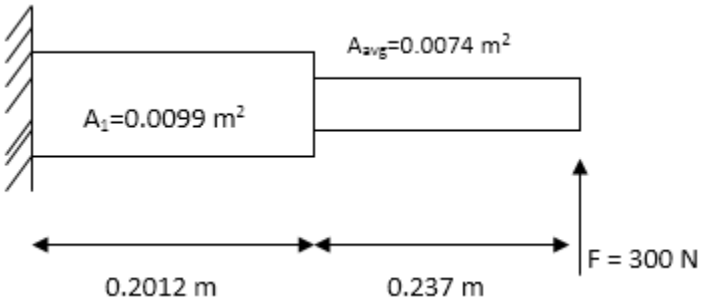

Figure A8. Support Structure Simplified Sketch

Average area of the second cross section has been calculated by taking the average of the minimum and maximum height of the second section. Maximum height = 0.131 m, minimum height = 0.064 m and width is constant at 0.0762 m. The total mass of the robot is 120 kg and using acceleration due to gravity to be 10 m/s^2, the total weight is 1200 N. Since there will be 4

such beams, the total force on 1 beam is 300 N. The material for the beam is steel with Young's modulus = 206.94 GPa [4].

The two sections of the beam have been treated as two beam members and the following stiffness matrix and equation was used to calculate the maximum deflection (point of force application).

$$\begin{matrix} F_{1y} \\ M_1 \\ F_{2y} \\ M_2 \\ F_{3y} \\ M_3 \end{matrix} = E \begin{matrix} \frac{12I_1}{L_1^3} & \frac{6I_1}{L_1^2} & -\frac{12I_1}{L_1^3} & \frac{6I_1}{L_1^2} & 0 & 0 \\ \frac{6I_1}{L_1^2} & \frac{4I_1}{L_1} & -\frac{6I_1}{L_1^2} & \frac{2I_1}{L_1} & 0 & 0 \\ -\frac{12I_1}{L_1^2} & -\frac{6I_1}{L_1^2} & \frac{12I_1}{L_1^3}+\frac{12I_2}{L_2^3} & -\frac{6I_1}{L_1^2}+\frac{6I_2}{L_2^2} & -\frac{12I_2}{L_2^3} & \frac{6I_2}{L_2^2} \\ \frac{6I_1}{L_1^2} & \frac{2I_1}{L_1} & -\frac{6I_1}{L_1^2}+\frac{6I_2}{L_2^2} & \frac{4I_1}{L_1}+\frac{4I_2}{L_2} & \frac{6I_2}{L_2^2} & \frac{2I_2}{L_2} \\ 0 & 0 & \frac{12I_2}{L_2^3} & -\frac{6I_2}{L_2^2} & \frac{12I_2}{L_2^3} & -\frac{6I_2}{L_2^2} \\ 0 & 0 & \frac{6I_2}{L_2^2} & \frac{2I_2}{L_2} & \frac{-6I_2}{L_2^2} & \frac{4I_2}{L_2} \end{matrix} \begin{matrix} d_{1y} \\ \theta_1 \\ d_{2y} \\ \theta_2 \\ d_{3y} \\ \theta_3 \end{matrix}$$

Using the boundary conditions as d_{1y} and $\theta_1 = 0$, and $F_{3y} = 300$ N, d_{2y} and d_{3y} were calculated to be $0.201x10^{-4}$ m and $0.228x10^{-4}$ m, respectively.

Computer FEA using NX

The part was simulated using NX 8.0 using the same boundary conditions. Shown below are the changes in deflection from the start till the end.

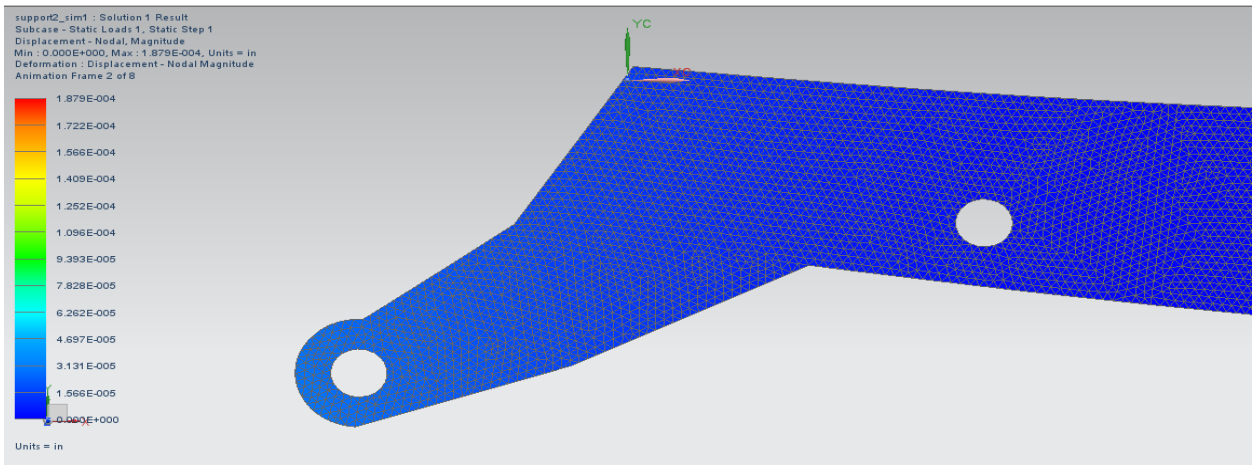

Figure A9. NX Analysis Initial State

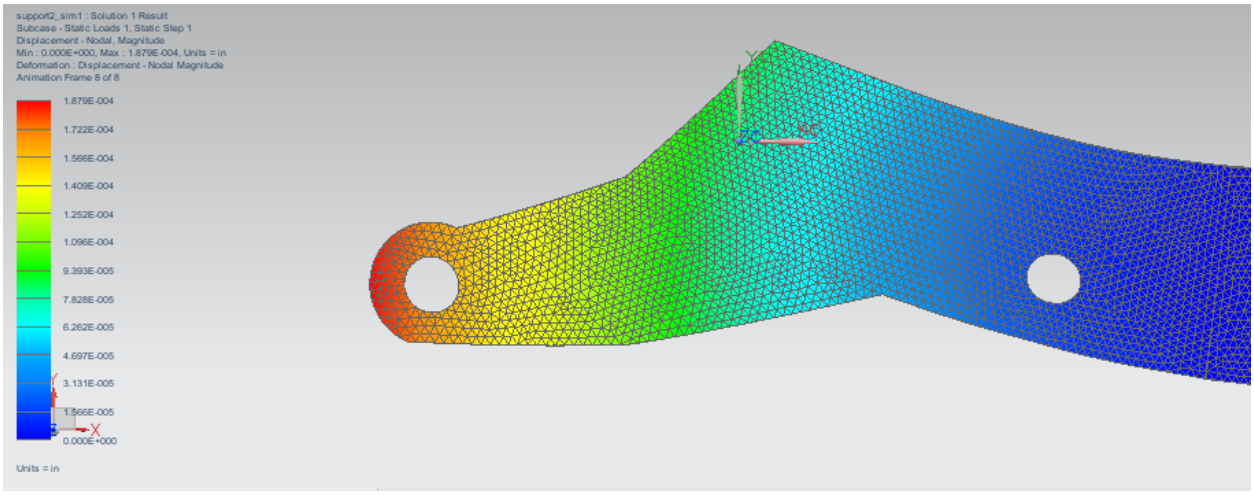

Figure A10. NX Analysis Final State

The maximum deflection obtained using NX was $0.477x10^{-5}$ m (the value in the figure is shown in inches). It was observed that the error between hand calculations and NX was significantly large and one of the main errors arose from the simplification of the geometry. The cross sectional area of the geometry is less than the simplified version, thus, will result in larger deflection. During hand calculations, only two beam elements were used whereas, in the simulation, the number of elements was in the order of 10^4. This can also cause significant error.

CONCLUSIONS AND FUTURE WORK

The objective of this project was to design a portable, all terrain, remote-controlled robot which will perform temperature and structural analysis. It would decrease the risk from a fire fighter's life by providing reconnaissance to the fire fighters of the chemical locations and weakening beams. Cameras used for these tasks: infrared for temperature sensing, synthetic aperture for seeing through smoke and high resolution color camera. Image analysis can be performed to determine the conditions of the structure. The robot will be connected to the fire hydrant for flame retardant purpose and also to cool the robot within operational temperatures. The designed robot will perform the required tasks like required traction, power transmission and suspension. However, there is much to be done regarding the sensing procedures and exact volumetric flow rates to keep the electronics cool. Future work includes working with electrical engineers to integrate the electronics and camera sensors, perform FEA on all components to determine the overall factor of safety and determine the production costs in manufacturing.

REFERENCES

[1] The Engineering Toolbox (2013). *Modulus of Rigidity of some Common Materials* [Online]. < http://www.engineeringtoolbox.com/modulus-rigidity-d_946.html>

[2] The Engineering Toolbox (2013). *Thermal Conductivity of some common materials and gases* [Online]. <http://www.engineeringtoolbox.com/thermal-conductivity-d_429.html>

[3] The Engineering Toolbox (2013). *Convective Heat Transfer* [Online]. <http://www.engineeringtoolbox.com/convective-heat-transfer-d_430.html>

[4] The Engineering Toolbox (2013). *Young Modulus for common materials* [Online]. <http://www.engineeringtoolbox.com/young-modulus-d_417.html>